

<sup>1</sup> Supplementary information for: Rural cropland abandonment is too  
<sup>2</sup> ephemeral to benefit carbon sequestration or biodiversity  
<sup>3</sup> conservation

<sup>4</sup> Christopher L. Crawford<sup>1\*</sup>    He Yin<sup>2</sup>    Volker C. Radeloff<sup>3</sup>    David S. Wilcove<sup>1,4</sup>

<sup>5</sup> <sup>1</sup>Princeton School of Public and International Affairs, Princeton University, Princeton, NJ

<sup>6</sup> <sup>2</sup>Department of Geography, Kent State University, Kent, OH

<sup>7</sup> <sup>3</sup>SILVIS Lab, Department of Forest & Wildlife Ecology, University of Wisconsin - Madison,  
<sup>8</sup> Madison, WI

<sup>9</sup> <sup>4</sup>Department of Ecology & Evolutionary Biology, Princeton University, Princeton, NJ

<sup>10</sup>  
<sup>11</sup> September 22, 2021

## <sup>12</sup> **Contents**

<sup>13</sup> <b>S1 Extended Results</b>	<sup>5</sup>
<sup>14</sup> S1.1 Limited abandonment in Mato Grosso . . . . .	<sup>5</sup>
<sup>15</sup> S1.2 Biomes . . . . .	<sup>5</sup>
<sup>16</sup> S1.3 The effect of varying abandonment definitions . . . . .	<sup>6</sup>
<sup>17</sup> S1.4 Comparing annual and two-year estimates of abandonment . . . . .	<sup>6</sup>
<sup>18</sup> S1.5 Maps of abandonment duration as of 2017 and maximum duration during time series . . . . .	<sup>7</sup>
<sup>19</sup> <b>S2 Extended Methods</b>	<sup>7</sup>
<sup>20</sup> S2.1 Classifying abandonment . . . . .	<sup>7</sup>
<sup>21</sup> S2.2 Temporal filters . . . . .	<sup>7</sup>
<sup>22</sup> S2.3 Modeling abandonment decay . . . . .	<sup>7</sup>
<sup>23</sup> S2.4 Change in recultivation rates over time . . . . .	<sup>9</sup>
<sup>24</sup> S2.5 Projecting abandonment duration into the future . . . . .	<sup>9</sup>
<sup>25</sup> <b>References</b>	<sup>10</sup>
<sup>26</sup> <b>S3 Supplementary Tables</b>	<sup>11</sup>
<sup>27</sup> <b>S4 Supplementary Figures</b>	<sup>12</sup>

---

\*Corresponding Author, [ccrawford@princeton.edu](mailto:ccrawford@princeton.edu), Robertson Hall, Princeton University, Princeton, NJ

<sup>28</sup> **List of Tables**

<sup>29</sup> S1	Summary statistics describing the duration of abandonment (in years) at our eleven sites between 1987 and 2017, using a five year abandonment definition, and incorporating all periods of abandonment (allowing for multiple per pixel). . . . .	11
<sup>32</sup> S2	Cropland abandonment (in Mha) as of 2017 as identified using a) our annual time series and a five-year abandonment definition and b) a two year method taking the difference between land cover in 1987 and 2017. . . . .	11

<sup>35</sup> **List of Figures**

<sup>36</sup> S1	The locations of our 11 sites, from Yin et al. <sup>6</sup> Sites are labeled as follows: (b) Vitebsk, Belarus / Smolensk, Russia; (bh) Bosnia & Herzegovina; (c) Chongqing, China; (g) Goiás, Brazil; (i) Iraq; (mg) Mato Grosso, Brazil; (n) Nebraska/Wyoming, USA; (o) Orenburg, Russia / Uralsk, Kazakhstan; (s) Shaanxi/Shanxi, China; (v) Volgograd, Russia; (w) Wisconsin, USA. . . . .	12
<sup>40</sup> S2	Area abandoned a) as of 2017, b) at any point between 1987-2017, c) as of 2017 as a proportion of the total cropland extent (i.e., the area of all lands that were cultivated at some point during the time series). Note that sites are shown in ascending order of area abandoned as of 2017 as a proportion of total cropland extent. . . . .	13
<sup>44</sup> S3	Cumulative area abandoned at each site through time, according to age class (in years). . . . .	14
<sup>45</sup> S4	Area in each land cover class at each site through time. Land cover classes are cropland, grassland, woody vegetation, non-vegetation, and abandoned (for at least 5 years). . . . .	15
<sup>47</sup> S5	Annual turnover of abandoned croplands at each site, showing the annual gain (dark green) and annual loss (i.e., recultivation, light green) and net change (black line) of abandoned croplands. . . . .	16
<sup>50</sup> S6	The distribution of the maximum abandonment duration (in years) for each pixel at each site from 1987 to 2017. The y-scale shows the proportion of pixels with maximum duration values of a given duration at each site. As previously noted, abandonment and recultivation can occur multiple times at a single pixel during our time series, and this figure serves as a companion to the distribution of all abandonment values shown in Figure 2. Site-level mean duration values are shown in the red and blue dots, corresponding to mean values calculated across all periods of abandonment (in red, including multiple periods per pixel) and mean values calculated across only the maximum duration of abandonment at each pixel (in blue). The vertical dashed lines represent the mean of these site-level mean duration values, for all abandonment periods (red) and only the maximum duration at each pixel (blue), respectively.	17
<sup>60</sup> S7	Maximum duration of cropland abandonment (in years) observed at each pixel between 1987 and 2017 in our eleven study sites. This serves as a companion to maps of the abandonment duration as of 2017 shown in Figure 1. Site locations are shown in Figure S1. . . . .	18
<sup>63</sup> S8	Proportion of abandoned cropland in each land cover class as of 2017. . . . .	19
<sup>64</sup> S9	Site biomes, using biome classifications from The Nature Conservancy's Terrestrial Ecoregions of The World (TEOW) database, derived from Olson et al. <sup>12</sup> and Olson and Dinerstein. <sup>13</sup> . .	20
<sup>66</sup> S10	Mean abandonment lengths shown for various abandonment thresholds. . . . .	21
<sup>67</sup> S11	Recultivation rates shown for various abandonment thresholds. . . . .	22

68	S12 Decay model results for all sites, showing the proportion of each cohort of abandoned land (i.e., all pixels abandoned in a given year) remaining abandoned over time for each of our eleven sites. Points represent actual observations by cohort, dashed lines represent linear model predictions (fitted values) for each cohort as a function of time (including a linear and logarithmic term of time), and the solid black line represents the site-level mean trend across all cohorts (calculated by taking the mean of each time coefficient values across all cohorts, respectively, and using those two mean values to plot a mean trend). Colors of both points and dashed lines correspond to roughly five-year group of cohorts, ranging from dark purple (oldest cohorts) to green and yellow (most recent cohorts). The horizontal black dashed line shows a proportion of 0.5, indicating the point where half of a cohort has been recultivated. Model diagnostic plots are shown in Figures S14 and S15. . . . .	23
79	S13 Akaike Information Criterion (AIC) values for various recultivation (“decay”) model specifica- tions for each site. More negative AIC values indicate a better model fit. . . . .	24
81	S14 Residuals vs. fitted diagnostic plots for our linear models of the recultivation (“decay”) of abandonment at each site. These models take the form shown in Equation (S2), and are shown in Figure S12. . . . .	25
84	S15 QQ plots calculated using the <code>{car}</code> package <sup>14</sup> for our linear models of the recultivation (“decay”) of abandonment at each site. These models take the form shown in Equation (S2), and are shown in Figure S12. . . . .	26
87	S16 Mean decay model coefficients across cohorts at each site. The left panel shows the mean coefficient on the log(time) terms and the right shows the site mean coefficient on the linear time terms. These mean coefficients are used to plot the mean decay trajectories shown in Figure 3. . . . .	27
91	S17 An alternative representation of the mean decay rate for each site (also shown in Figure 3). The color of each point corresponds to the proportion remaining after a given amount of time. . . . .	28
93	S18 The rate of change of decay rates (measured as the half-life, or the time required for 50% of each cohort to be recultivated) at each site over the course of the time series. Individual site trends are shown in panel a. Solid lines show simple linear regressions, the slopes of which are shown in panel b. Gray bands around the linear trends in panel a and the error bars on slope estimates in panel b both represent 95% confidence intervals. These models are described by Eq. (S3). Model diagnostic plots are shown in Figures S19 and S20. . . . .	29
99	S19 Residuals vs. fitted diagnostic plots for each site, for a simple <code>lm</code> call corresponding to Eq. (S3), in which the half-life (i.e., the time required for half (50%) of a given cohort of abandoned cropland to be recultivated) is modeled as a function of the year of initial abandonment at each site. . . . .	30
103	S20 QQ plots calculated using the <code>car</code> package <sup>(14)</sup> , for a simple <code>lm</code> call corresponding to Eq. (S3), in which the half-life (i.e., the time required for half (50%) of a given cohort of abandoned cropland to be recultivated) is modeled as a function of the year of initial abandonment at each site. . . . .	31
107	S21 Annual gain in newly abandoned cropland at our eleven sites. Panel a shows the trend in annual abandonment over time at each site (in $10^3$ ha), and Panel b shows the mean annual abandonment (in $10^3$ ha) at each site. The mean values in panel b feed into the extrapolations. Note that the annual gain in abandonment corresponds to the dark green bars in Figure S5. . . . .	32
111	S22 The results of our simple extrapolation, including a) the mean age of abandonment, and b) the total area abandoned into the future. Colors corresponding to each site are consistent across the three panels. These extrapolation assume recultivation based on the mean decay trend for each site Figure 3 and annual new abandonment based on the mean annual gain in abandonment shown in Figure S5 (dark green bars). . . . .	32

116	S23 Extrapolating area by age bin, assuming a 1) each site follows the mean recultivation (“decay”) 117 rate, and 2) a constant area abandoned each year (based on the mean annual area abandoned 118 at each site). . . . .	33
119	S24 The results of our second extrapolation, including a) the mean age of abandonment, and b) 120 the total area abandoned into the future. Colors corresponding to each site are consistent 121 across the three panels. These extrapolation assume recultivation based on the mean decay 122 trend for each site Figure 3 and annual new abandonment based on the mean annual gain in 123 abandonment shown in Figure S5 (dark green bars). . . . .	34
124	S25 Extrapolating area by age bin, assuming a 1) each site follows the mean recultivation (“decay”) 125 rate, and 2) a constant area abandoned each year until 2017 (based on the mean annual 126 area abandoned at each site), followed by a linearly declining area abandoned each year until 127 reaching 0 in 2050. . . . .	35
128	S26 Comparing the mean duration of abandonment at our 11 sites observed between 1987 and 129 2017 with the extrapolated mean duration as of 2050 for our two extrapolations. . . . .	36
130	S27 Abandonment patterns for Vitebsk, Belarus / Smolensk, Russia, showing a) accumulation of 131 abandoned land by age class, b) decay of abandoned land by year abandoned, c) the area in 132 each land cover class through time (including both land that has been abandoned for five or 133 more years, as well as any land abandoned for 1 or more years, therefore including short-term 134 fallows), d) the annual turnover of abandoned land through time, and e) the distribution 135 of abandonment duration for all periods of cropland abandonment (top) and the maximum 136 duration of abandonment at each pixel (bottom). . . . .	37
137	S28 Abandonment patterns for Bosnia & Herzegovina, following Figure S27. . . . .	38
138	S29 Abandonment patterns for Chongqing, China, following Figure S27. . . . .	39
139	S30 Abandonment patterns for Goiás, Brazil, following Figure S27. . . . .	40
140	S31 Abandonment patterns for Iraq, following Figure S27. . . . .	41
141	S32 Abandonment patterns for Mato Grosso, Brazil, following Figure S27. . . . .	42
142	S33 Abandonment patterns for Nebraska/Wyoming, USA, following Figure S27. . . . .	43
143	S34 Abandonment patterns for Orenburg, Russia / Uralsk, Kazakhstan, following Figure S27. . .	44
144	S35 Abandonment patterns for Shaanxi/Shanxi, China, following Figure S27. . . . .	45
145	S36 Abandonment patterns for Volgograd, Russia, following Figure S27. . . . .	46
146	S37 Abandonment patterns for Wisconsin, USA, following Figure S27. . . . .	47

## <sup>147</sup> S1 Extended Results

<sup>148</sup> Cropland abandonment at individual sites (excluding Mato Grosso, see Section S1.A.) ranged between  
<sup>149</sup> 314,374.8 ha (Shaanxi) and 930,424 ha (Orenburg) as of 2017 (Figure S3), and because our sites varied in  
<sup>150</sup> size, this corresponded to between 7.91% (Nebraska) and 19.91% (Shaanxi) of the total area of each site  
<sup>151</sup> (Figure S2).

<sup>152</sup> On average, we found that cropland abandonment lasted for only 14.42 years ( $SD = 1.52$  years) across our  
<sup>153</sup> time series at our eleven sites. Note, however, that these summary statistics are calculated based on the  
<sup>154</sup> mean abandonment duration at each site, to account for different site sizes. The summary statistics reported  
<sup>155</sup> are therefore the mean of the mean abandonment duration at each of our eleven sites, and the standard  
<sup>156</sup> deviation of the mean abandonment duration at each of our eleven sites.

<sup>157</sup> We also calculated the mean standard deviation of abandonment duration across our sites, which was 7.78  
<sup>158</sup> years. The former is a measure of the spread of mean abandonment lengths across the 11 sites, whereas the  
<sup>159</sup> latter is a measure of the average spread of abandonment lengths at each site. See Table S1.

<sup>160</sup> The area abandoned at each site is shown in Figure S2 (see also Table S2). The area abandoned at each site,  
<sup>161</sup> by age class, is shown in Figure S3, and the area in each land cover class at each site is shown in Figure S4.  
<sup>162</sup> Figure S3 shows that the timing of abandonment varied across sites; some sites showed more abandonment  
<sup>163</sup> earlier in the time series (e.g., Iraq; Bosnia & Herzegovina; Volgograd, Russia; Nebraska/Wyoming, USA;  
<sup>164</sup> & Mato Grosso, Brazil), some showed consistent abandonment over time (e.g., Vitebsk, Belarus/Smolensk,  
<sup>165</sup> Russia; Goiás, Brazil; and Wisconsin, USA), and others showed increasing abandonment later on in the time  
<sup>166</sup> series (e.g., sites in Shaanxi/Shanxi and Chongqing, China). Furthermore, Figure S5 shows the annual gain,  
<sup>167</sup> loss, and net change in the area of abandoned croplands abandoned at each site.

### <sup>168</sup> S1.1 Limited abandonment in Mato Grosso

<sup>169</sup> Mato Grosso, Brazil, was the only site that did not experience significant amounts of cropland abandonment  
<sup>170</sup> during our time series. This is unsurprising given the recent history of agriculturally-driven land-use change  
<sup>171</sup> over the last few decades. That being said, the abandonment that did take place in Mato Grosso was relatively  
<sup>172</sup> more durable, requiring 25 years to decline by half and 110 years for complete turnover. However, because  
<sup>173</sup> Mato Grosso showed large amounts of new cultivation over the source of our time series and relatively little  
<sup>174</sup> abandonment (9,006 ha, or 0.47% of the total cropland extent, as of 2017), these results should be interpreted  
<sup>175</sup> with care.

### <sup>176</sup> S1.2 Biomes

<sup>177</sup> Some ecosystems and biomes seem to recover more quickly than others, namely in relatively higher latitudes,  
<sup>178</sup> relatively colder climates, and in relatively more humid biomes.<sup>1</sup> Our sites cover a range of biomes (Figure  
<sup>179</sup> S9), including:

- <sup>180</sup> • Temperate Broadleaf and Mixed Forests (Vitebsk Belarus/Smolensk, Russia; Bosnia & Herzegovina;  
<sup>181</sup> Wisconsin, USA),
- <sup>182</sup> • Temperate Grasslands, Savannas, and Shrublands (Nebraska/Wyoming, USA; Orenburg, Russia/Uralsk,  
<sup>183</sup> Kazakhstan; Volgograd, Russia),
- <sup>184</sup> • Tropical Grassland (Goiás and Mato Grosso, Brazil),
- <sup>185</sup> • Tropical Moist Broadleaf Forests (Chongqing, China; Mato Grosso, Brazil),
- <sup>186</sup> • Montane Grassland and Shrublands (Shaanxi/Shanxi, China), and
- <sup>187</sup> • Deserts & Xeric Shrublands (Iraq).

<sup>188</sup> The long-term land-cover outcomes for abandoned croplands are shown (as of 2017) in Figure S8. Land cover  
<sup>189</sup> outcomes for abandoned croplands showed wide variation across sites, with most abandonment in Wisconsin

190 being classified as forest by 2017 (60% forest, 40% grassland), but remaining mostly in grassland elsewhere  
191 (Figure S8). This limited woody vegetation regrowth may be a product of the biome, but it may simply be a  
192 result of insufficient time for woody biomass to develop. Land cover alone cannot confidently serve as a proxy  
193 for ecosystem recovery.

### 194 **S1.3 The effect of varying abandonment definitions**

195 A relatively short-term definition of abandonment might result in an overestimation of recultivation, because  
196 short-term abandonment may be better understood as cyclical fallow periods, not true abandonment.<sup>2</sup>  
197 Because typical fallow period length may vary around the world, we tested multiple abandonment thresholds  
198 in order to test the sensitivity of our results to our choice of a five-year abandonment definition, following the  
199 FAO.<sup>3</sup> As our abandonment threshold increased in length, the mean abandonment duration across our sites  
200 increased accordingly, ranging between 7 years (no threshold) and 19 years (10-year threshold). As expected,  
201 using a longer abandonment definition reduced the amount of cropland abandonment we detected, which is  
202 also shown in the area in the different colored age classes in Figure S3.

203 The proportion of abandoned croplands that were recultivated by the end of the time series also responded to  
204 our abandonment threshold, with less recultivation for longer abandonment thresholds (Figure S11). However,  
205 even at the longest abandonment definition (10 years), we still saw that between 10% and 30% of abandoned  
206 croplands were recultivated by the end of the time series. We find that the mean area of abandoned croplands  
207 that get recultivated by the end of the time series declines from 37.77% with a 5 year threshold to 30.93%  
208 with a 7 year threshold, and 22.83% with a 10 year threshold. This indicates that the abandonment and  
209 recultivation we observe is not merely a function of our five-year abandonment definition.

### 210 **S1.4 Comparing annual and two-year estimates of abandonment**

211 Some studies estimate cropland abandonment by simply looking for areas where land cover is classified as  
212 “cultivated” in one year, but not in a later year (e.g., 1992 and 2015 in ref.).<sup>4</sup> In order to understand the  
213 magnitude of the differences that could result from using this two-year approach, we estimated cropland  
214 abandonment by simply identifying areas that were classified as “cropland” in 1987 and classified as either  
215 “woody vegetation” or “herbaceous vegetation” in 2017 (i.e., excluding “non-vegetation”).

216 Table S2 shows the area of abandoned croplands as identified using a five-year abandonment definition and the  
217 full annual time series (Column 2), and the area of abandoned croplands identified using only the difference  
218 between 2017 and 1987 (Column 3). These two methods produced abandonment area estimates that ranged  
219 between 39.75% lower (Goiás, Brazil) and 83.29% higher (Mato Grosso, Brazil) than the abandoned area  
220 identified using the full time series.

221 Not only do these methods produce different area estimates, but they also differ in the location of the  
222 abandonment they identify, with spatial agreement of only 28.08% (Mato Grosso, Brazil) to 66.3% (Bosnia &  
223 Herzegovina) (see Table S2). We measure spatial agreement using the Jaccard similarity index [Legendre2012],  
224 a measure of overlap between two sets, defined as the proportion of shared elements, or the intersection  
225 divided by the union (Equation (S1)):<sup>5</sup>

$$J(a, b) = \frac{a \cap b}{a \cup b} \quad (\text{S1})$$

226 Additionally, a large portion of the “abandoned” area identified with the two-year method does not meet our  
227 five year abandonment definition, leading to an overestimate of true abandonment. Column 6 in Table S2  
228 shows the percent of the “abandoned” area identified with the two-year method that has been abandoned for  
229 more than 5 years, and therefore would not be considered “abandoned” by our definition.

230 **S1.5 Maps of abandonment duration as of 2017 and maximum duration during  
231 time series**

232 As described in the main text, because a pixel may be abandoned and recultivated multiple times throughout  
233 the time series, we calculated the mean abandonment duration in two ways: 1) across all periods of  
234 abandonment (as shown in Figure 2), and 2) across only the longest period of abandonment experienced by  
235 each pixel. Maps of the maximum abandonment duration at each pixel at each site is shown in Figure S7  
236 (serving as a companion to Figure 1). The distribution of maximum duration values, and the corresponding  
237 mean maximum duration value at each site, is shown in Figure S6 (serving as a companion to Figure 2).

238 Expanded site-specific results are shown in Figures S27-S37.

239 **S2 Extended Methods**

240 As noted in our main text, we build on annual land cover maps for 1987-2017 developed by Yin et al.<sup>6</sup>  
241 The following section outlines our data processing and analytical methods in more specific detail than was  
242 possible in the main text. We processed and analyzed our abandonment map data in RStudio version  
243 1.4.1717,<sup>7</sup> using R version 4.1.0 (2021-05-18), relying heavily on the `{raster}`,<sup>8</sup> `{terra}`,<sup>9</sup> `{data.table}`,<sup>10</sup>  
244 and `{tidyverse}`<sup>11</sup> packages.

245 **S2.1 Classifying abandonment**

246 Pixels that remained in cropland or non-cropland classes throughout the entire time series were excluded,  
247 as were periods of non-cropland that began in the first year of the time series, even if that pixel was later  
248 classified as cropland and subsequently abandoned. In effect, we only counted periods of abandonment that  
249 we could verify had followed agricultural activity during our time series.

250 As noted, pixels that transitioned from cropland to the non-vegetation land cover class were not considered  
251 “abandoned,” and therefore we excluded all non-vegetation pixels from our entire analysis. These pixels  
252 accounted for <10% of total site area at all sites except Shaanxi (12.7%) and Iraq (52.8%), and remained  
253 stable or declined over time at all eleven sites (see Figure S4).

254 All area calculations were performed using the `{terra}` package’s `cellSize()` function, which calculates the  
255 spherical area of each cell as defined by its four corners.<sup>9</sup>

256 **S2.2 Temporal filters**

257 In order to address potential classification errors in a single year, we implemented a series of temporal filters  
258 designed to smooth trajectories by looking for short-term land-cover changes that are temporally unlikely.  
259 We applied five-year and eight-year moving-window filters that searched for short periods of land cover  
260 classifications that do not match those immediately before and after, and subsequently updated them to match  
261 the surrounding classifications. Specifically, the five-year filter searched for one year periods that did not  
262 match the two years immediately before and after (i.e., patterns of 11011, where 1 represents non-cropland  
263 and 0 represents cropland), and our eight-year filter searched for two year periods that did not match the  
264 three years before and after (i.e., 11100111). The central classifications were then updated to match the  
265 classes on either end.

266 **S2.3 Modeling abandonment decay**

267 Our mean abandonment duration metric tells us about the general persistence of abandoned croplands  
268 throughout the time series. However, this value is limited by the time series length, and does not account for

when the majority of the abandonment took place at a site, nor whether a period of abandonment ends as a result of recultivation or the end of the time series. As a result, the mean abandonment duration does not tell us how long to expect a piece of land to remain abandoned, nor how abandonment length varies through time. To address this constraint, we track the trajectory of each pixel through time following its initial abandonment, grouping pixels abandoned in a given year into “cohorts.” Decay rates provide information about how long it takes for land to be recultivated, complementing the mean abandonment length and providing a more nuanced story about how long to expect abandonment to last.

For example, a site may have a relatively short mean length of abandonment (e.g., Shaanxi/Shanxi [China], with a mean abandonment length of 13 years; see Figure 1), but also have a gradual decay rate, indicating that land should stay abandoned for a relatively longer amount of time. This may result from more abandonment occurring towards the end of the time series; this land simply does not have as long to age and shows up as younger in our data, regardless of how long it may last. Looking at abandonment decay rates for each cohort individually allows us to produce a decay rate for each site in general in a way that accounts for when during the time series a piece of land was abandoned (i.e., giving us a sense of how long to expect a given piece of land to remain abandoned, even into the future).

### S2.3.1 Model selection and diagnostics

We fit linear models using the `lm()` function in R’s core statistics package `{stats}`, predicting the proportion of abandoned cropland in each cohort remaining abandoned as a function of time since initial abandonment at each site ( $n = 351$  observations for each of our 11 sites). The proportion of abandoned cropland remaining abandoned is measured relative to the area abandoned 5 years following the year of initial abandonment, as dictated by our five year abandonment definition.

We tested a range of model specifications, including linear and log transformations of both *proportion* and *time*. Due to a linear relationship between model residuals and time when including only one term for *time*, we also tested models containing multiple *time* predictor terms, including both log and linear terms.

We chose a model with the following specifications shown in Equation 1 and reproduced here in Equation (S2). For cohorts of abandonment initially abandoned in years  $y = 1988, \dots, 2013$ , we estimate the proportion  $p$  of each cohort  $y$  remaining abandoned as a function of time  $t$  (i.e., based on the number of years after initial abandonment).

$$p_y = 1 + \beta_{1,y} \log(t + 1) + \beta_{2,y} t \quad (\text{S2})$$

Where  $\beta_{1,y}$  represents the regression coefficient on the log term of time  $t$  for cohort  $y$ , and  $\beta_{2,y}$  represents the regression coefficient on the linear term of time  $t$  for cohort  $y$ . We allow for *cohort* level fixed effects, fitting unique coefficients for each cohort at each site. We ran individual models for each site, using a `stats::lm()` call of `lm(formula = I(proportion - 1) ~ 0 + log(time + 1):cohort + I(time):cohort)` on data for only that site. Taken together, these 11 models correspond to a `stats::lm()` call of `lm(formula = I(proportion - 1) ~ 0 + log(time + 1):cohort:site + I(time):cohort:site)`.

Model selection was performed based on Akaike Information Criterion (AIC) values (Figure S13), selecting the model with the lowest (i.e., more negative) AIC value. We confirmed that linear model assumptions were not violated through visual inspection of both residuals vs. fitted plots (Figure S14) and Q-Q plots (Figure S15).

### S2.3.2 Recultivation (“decay”) model results

The observed data, fitted values from these linear models, and mean decay rates for each site, are shown in Figure S12.

In order to calculate the mean decay trajectory at each site (as shown in Figure 3), we took the mean of the log coefficients ( $\beta_{1,\bar{y}}$ ) and the linear coefficients ( $\beta_{2,\bar{y}}$ ) respectively across all cohorts  $y$  at each site. These

312 mean values are shown in Figure S16. We then used these mean coefficient values ( $\beta_{1,\bar{y}}$  and  $\beta_{1,\bar{y}}$ ) to define  
313 a new function describing the mean recultivation (or decay) trajectory at each site, using the same for as  
314 Equation (S2).

315 An alternative representation of the mean recultivation rate is shown in Figure S17.

### 316 **S2.4 Change in recultivation rates over time**

317 We examined the rate of change of recultivation rates by calculating the half-life,  $t_{half,s}$ , defined as the time  
318 required for half (50%) of a given cohort of abandoned cropland to be recultivated, and parameterizing a  
319 simple linear model on these half-life values as a function of time, using the `stats::lm()` function in R's  
320 core statistics package `{stats}`. This resulted in  $n = 26$  half-life values (one for each cohort) at each of our  
321 11 sites. We estimate the half-life,  $t_{half,s}$ , as a function of the year of initial abandonment ( $yearabn_s$ ), at  
322 each site  $s$ , as shown in Equation (S3).

$$t_{half,s} = \beta_{0,s} + \beta_{1,s} yearabn_s \quad (S3)$$

323 Where  $\beta_{1,s}$  represents the regression slope on the year abandoned (cohort) for site  $s$  ( $yearabn_s$ ), and  $\beta_{0,s}$  repre-  
324 sents the intercept. This corresponds to a `stats::lm()` call of `lm(formula = t_half ~ year_abandoned)`,  
325 run for each site individually. Results are shown in Figure S18.

326 We confirmed that model assumptions were met through visual inspection of residuals vs. fitted plots (Figure  
327 S19) and Q-Q plots (Figure S20).

### 328 **S2.5 Projecting abandonment duration into the future**

329 The results of the projection highlighted in the main text (referred to here as “Extrapolation 1”) are shown in  
330 Figure S22 and Figure S23. As noted in the main text, we make two simple assumptions in our projection of  
331 abandonment and recultivation into the future: specifically, that 1) recultivation rates remain the same (based  
332 on mean recultivation trends at each site, shown in Figure 3, and that 2) a constant amount of cropland is  
333 newly abandoned each year, based on the mean annual gain in abandonment shown in Figure S21b (note:  
334 the annual gain in abandonment in Figure S21a corresponds to the dark green bars in Figure S5).

335 Given that abandonment may not continue indefinitely, we also explore an alternative to our second assumption  
336 about the amount of additional abandonment each year. In this alternative assumption (“Extrapolation 2”),  
337 the area abandoned each year is the same as “Extrapolation 1” from 1987-2017, based on the mean annual  
338 gain in abandonment (Figure S21b), but linearly declines between 2017-2050, reaching 0 ha at each site in  
339 2050 (see Figures S24 and S25).

340 While mean age of abandoned land increased through time after 2017 (and most dramatically after 2050),  
341 it remained below 37 years at all sites by 2050. Increases in mean abandonment duration were offset by  
342 recultivation, and total area abandoned declined quickly after 2020 at most sites. The mean abandonment  
343 duration increases as annual abandonment declines, as the total pool of abandoned land grows older and is  
344 gradually recultivated.

345 **References**

- 346 1. Prach, K. & Walker, L. R. Differences between primary and secondary plant succession among biomes  
347 of the world. *Journal of Ecology* 510–516 (2018) doi:[10.1111/1365-2745.13078](https://doi.org/10.1111/1365-2745.13078).
- 348 2. Munroe, D. K., Berkel, D. B. van, Verburg, P. H. & Olson, J. L. Alternative trajectories of land  
349 abandonment: Causes, consequences and research challenges. *Current Opinion in Environmental  
Sustainability* 5, 471–476 (2013).
- 350 3. Food and Agriculture Organization of the United Nations (FAO). FAOSTAT Statistical Database:  
351 Methods & Standards. (2016).
- 352 4. Næss, J. S., Cavalett, O. & Cherubini, F. The land–energy–water nexus of global bioenergy potentials  
353 from abandoned cropland. *Nature Sustainability* (2021) doi:[10.1038/s41893-020-00680-5](https://doi.org/10.1038/s41893-020-00680-5).
- 354 5. Legendre, P. & Legendre, L. *Numerical ecology*. 990 (Boston: Elsevier, 2012).
- 355
- 356 6. Yin, H. *et al.* Monitoring cropland abandonment with Landsat time series. *Remote Sensing of  
357 Environment* 246, 111873 (2020).
- 358 7. RStudio Team. RStudio: Integrated Development Environment for R. (2020).
- 359
- 360 8. Hijmans, R. J. *Raster: Geographic data analysis and modeling*. (2021).
- 361
- 362 9. Hijmans, R. J. *Terra: Spatial data analysis*. (2021).
- 363
- 364 10. Dowle, M. & Srinivasan, A. *Data.table: Extension of ‘data.frame’*. (2021).
- 365
- 366 11. Wickham, H. *Tidyverse: Easily install and load the tidyverse*. (2021).
- 367
- 368 12. Olson, D. M. *et al.* Terrestrial Ecoregions of the World: A New Map of Life on Earth. *BioScience* 51,  
369 933–938 (2001).
- 370 13. Olson, D. M. & Dinerstein, E. The Global 200: Priority ecoregions for global conservation. *Annals of  
371 the Missouri Botanical Garden* 89, 199–224 (2002).
- 372 14. Fox, J., Weisberg, S. & Price, B. *Car: Companion to applied regression*. (2021).
- 373

### <sup>374</sup> S3 Supplementary Tables

Table S1: Summary statistics describing the duration of abandonment (in years) at our eleven sites between 1987 and 2017, using a five year abandonment definition, and incorporating all periods of abandonment (allowing for multiple per pixel).

	Site	Mean	Median	Standard Deviation
Vitebsk, Belarus / Smolensk, Russia		13.87	12	7.60
Bosnia & Herzegovina		17.70	18	8.36
Chongqing, China		12.92	11	7.32
Goiás, Brazil		13.61	12	7.42
Iraq		15.72	13	8.78
Mato Grosso, Brazil		15.30	11	9.21
Nebraska/Wyoming, USA		15.32	14	8.04
Orenburg, Russia / Uralsk, Kazakhstan		12.86	11	6.95
Shaanxi/Shanxi, China		13.00	11	7.15
Volgograd, Russia		13.33	12	7.01
Wisconsin, USA		15.00	14	7.78

Table S2: Cropland abandonment (in Mha) as of 2017 as identified using a) our annual time series and a five-year abandonment definition and b) a two year method taking the difference between land cover in 1987 and 2017.

	Site	Area (annual, as of 2017)	Area (two year: 2017-1987)	Percent Difference	Jaccard Similarity	Percent Area <5 Years Old (two year)
Goiás, Brazil		530,252	319,499	-39.75%	0.29	22.61%
Vitebsk, Belarus / Smolensk, Russia		917,934	655,689	-28.57%	0.51	16.71%
Chongqing, China		382,125	273,839	-28.34%	0.43	25.19%
Nebraska/Wyoming, USA		351,006	274,133	-21.9%	0.50	15.47%
Bosnia & Herzegovina		690,376	569,091	-17.57%	0.66	10.18%
Wisconsin, USA		411,833	358,420	-12.97%	0.48	28.32%
Iraq		368,103	348,152	-5.42%	0.54	22.7%
Volgograd, Russia		828,276	857,989	3.59%	0.47	32.77%
Orenburg, Russia / Uralsk, Kazakhstan		930,424	975,131	4.8%	0.52	28.81%
Shaanxi/Shanxi, China		314,375	355,581	13.11%	0.49	27.21%
Mato Grosso, Brazil		9,006	16,507	83.29%	0.28	0.52%

<sup>375</sup> S4 Supplementary Figures

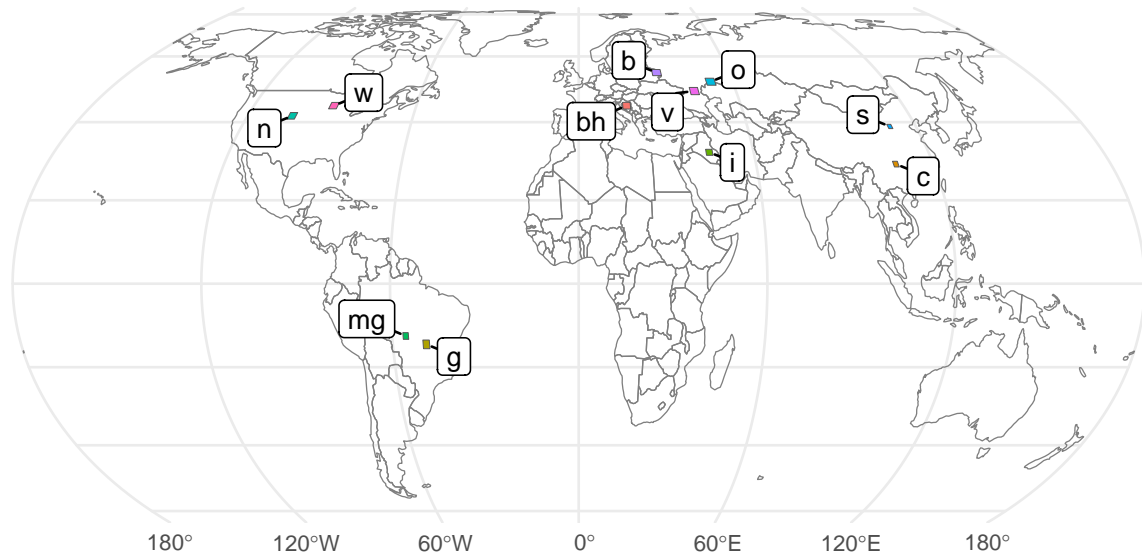


Figure S1: The locations of our 11 sites, from Yin et al.<sup>6</sup> Sites are labeled as follows: (b) Vitebsk, Belarus / Smolensk, Russia; (bh) Bosnia & Herzegovina; (c) Chongqing, China; (g) Goiás, Brazil; (i) Iraq; (mg) Mato Grosso, Brazil; (n) Nebraska/Wyoming, USA; (o) Orenburg, Russia / Uralsk, Kazakhstan; (s) Shaanxi/Shanxi, China; (v) Volgograd, Russia; (w) Wisconsin, USA.

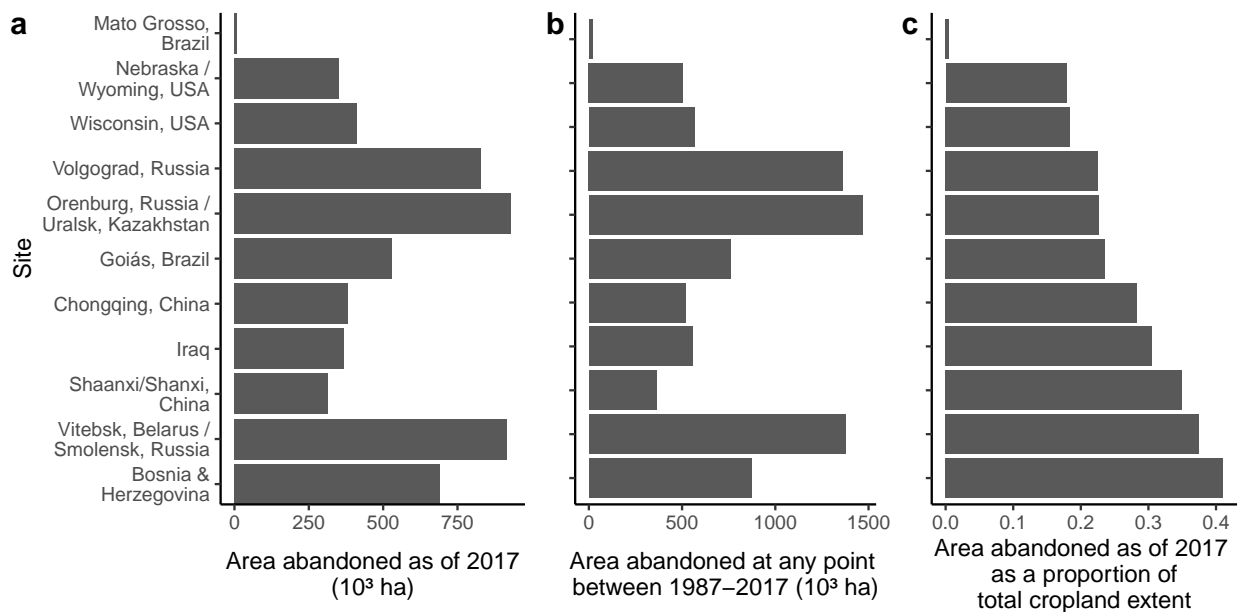


Figure S2: Area abandoned a) as of 2017, b) at any point between 1987–2017, c) as of 2017 as a proportion of the total cropland extent (i.e., the area of all lands that were cultivated at some point during the time series). Note that sites are shown in ascending order of area abandoned as of 2017 as a proportion of total cropland extent.

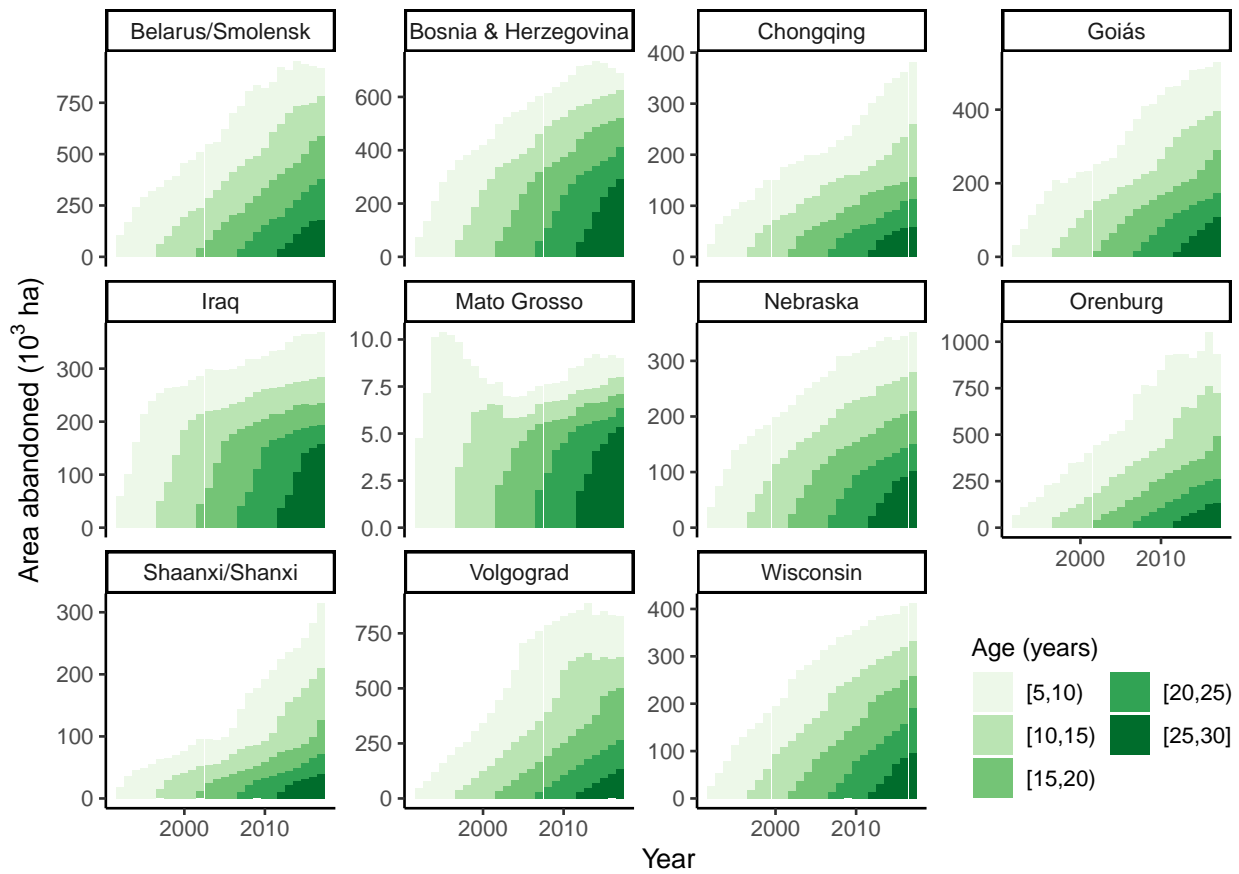


Figure S3: Cumulative area abandoned at each site through time, according to age class (in years).

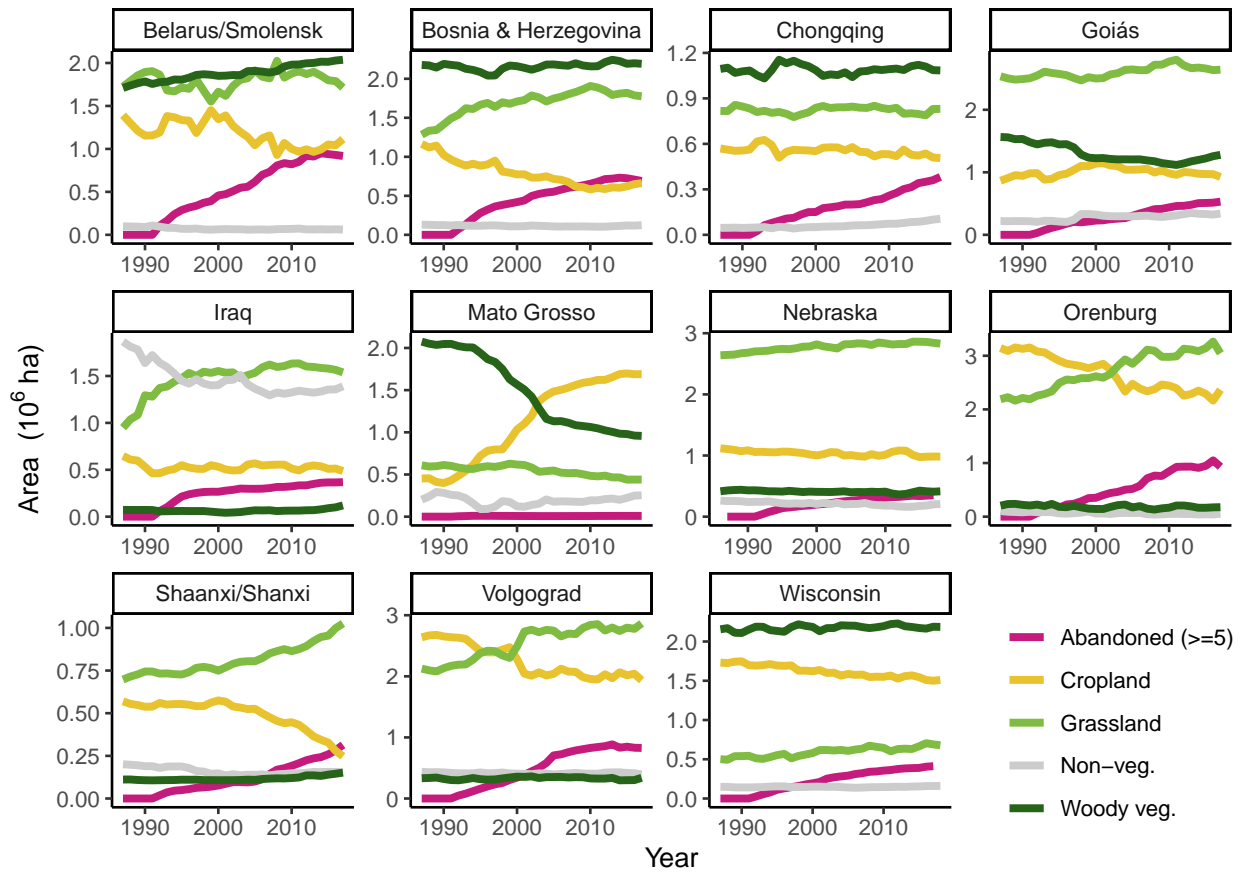


Figure S4: Area in each land cover class at each site through time. Land cover classes are cropland, grassland, woody vegetation, non-vegetation, and abandoned (for at least 5 years).

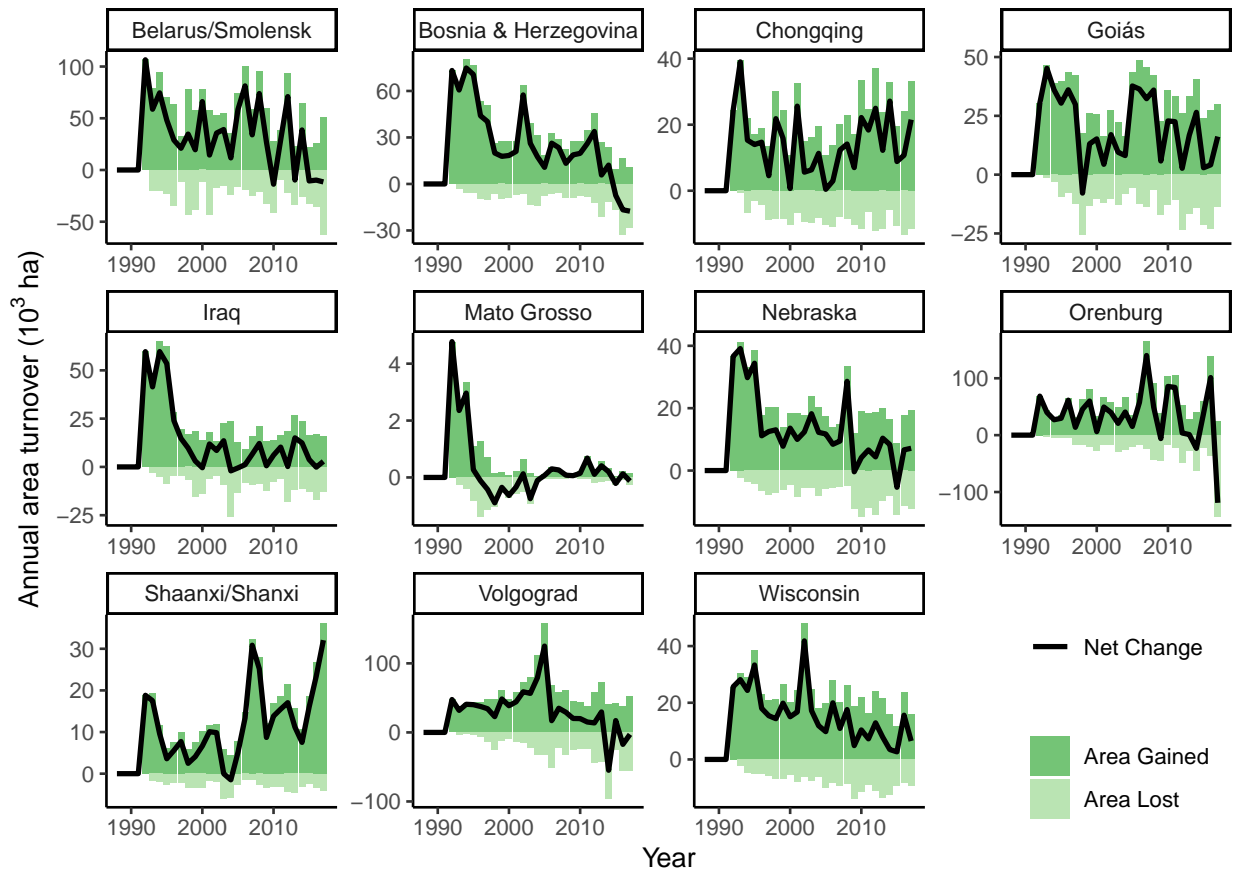


Figure S5: Annual turnover of abandoned croplands at each site, showing the annual gain (dark green) and annual loss (i.e., recultivation, light green) and net change (black line) of abandoned croplands.

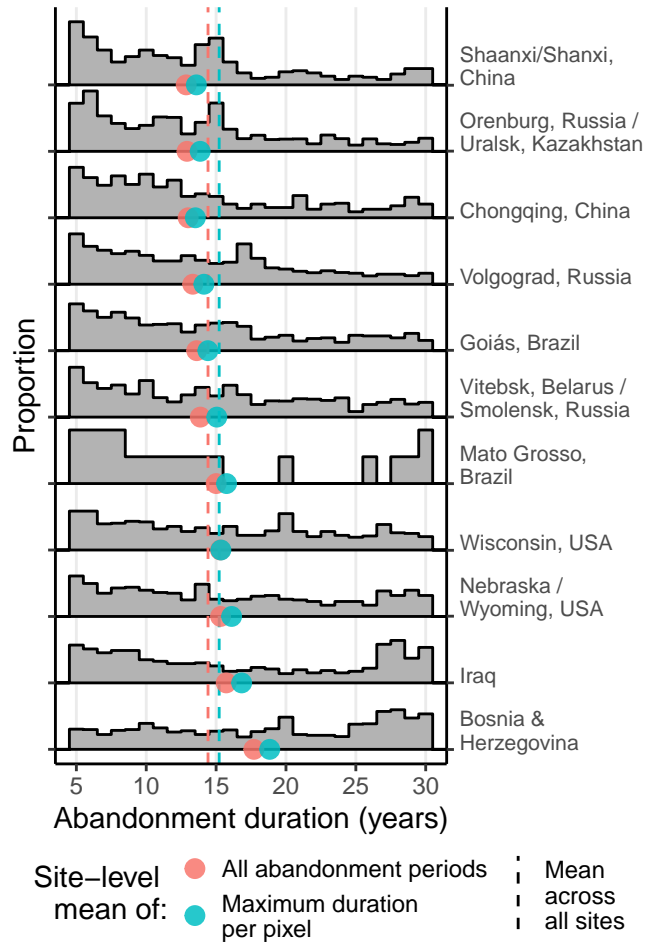


Figure S6: The distribution of the maximum abandonment duration (in years) for each pixel at each site from 1987 to 2017. The y-scale shows the proportion of pixels with maximum duration values of a given duration at each site. As previously noted, abandonment and recultivation can occur multiple times at a single pixel during our time series, and this figure serves as a companion to the distribution of all abandonment values shown in Figure 2. Site-level mean duration values are shown in the red and blue dots, corresponding to mean values calculated across all periods of abandonment (in red, including multiple periods per pixel) and mean values calculated across only the maximum duration of abandonment at each pixel (in blue). The vertical dashed lines represent the mean of these site-level mean duration values, for all abandonment periods (red) and only the maximum duration at each pixel (blue), respectively.

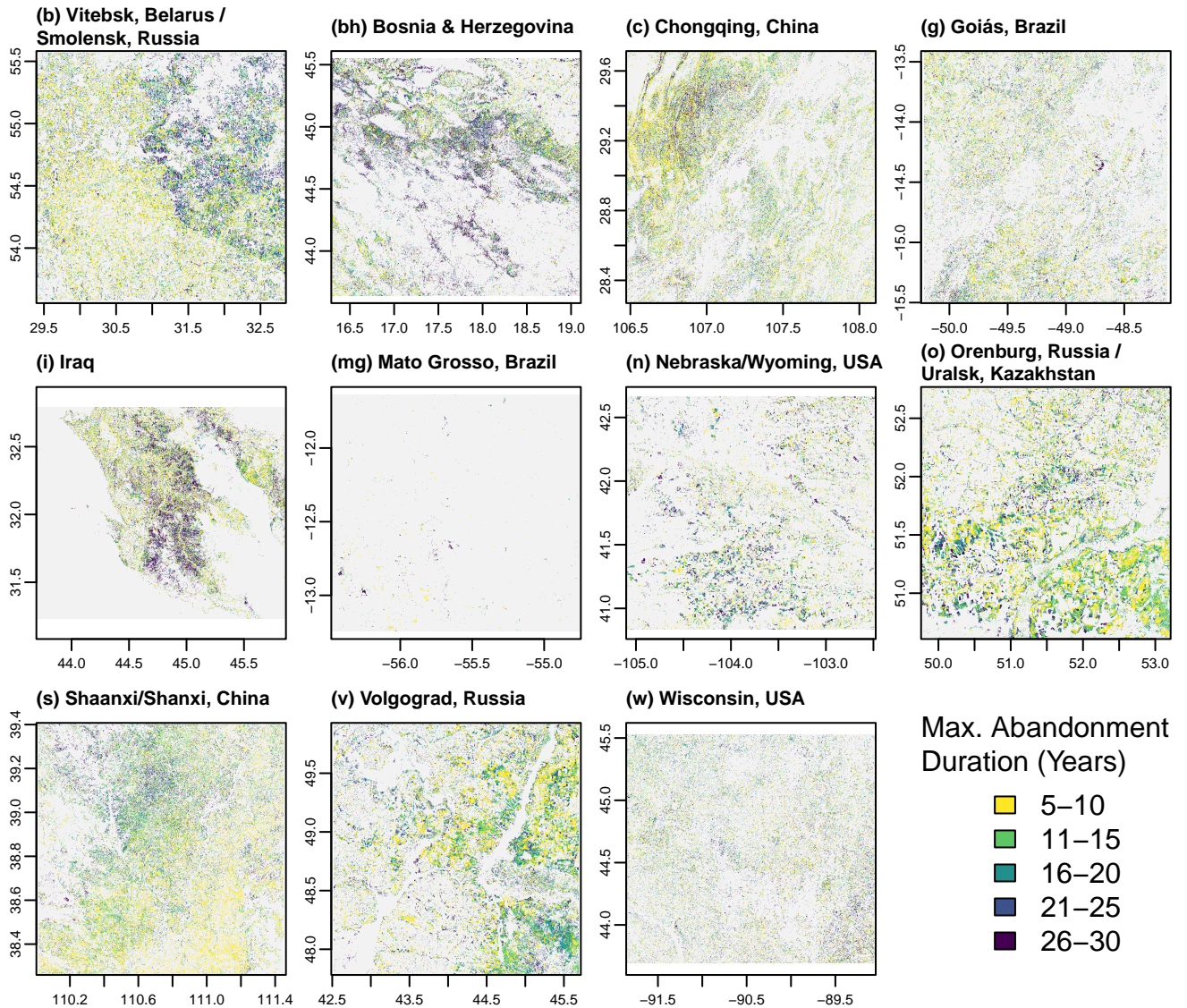


Figure S7: Maximum duration of cropland abandonment (in years) observed at each pixel between 1987 and 2017 in our eleven study sites. This serves as a companion to maps of the abandonment duration as of 2017 shown in Figure 1. Site locations are shown in Figure S1.

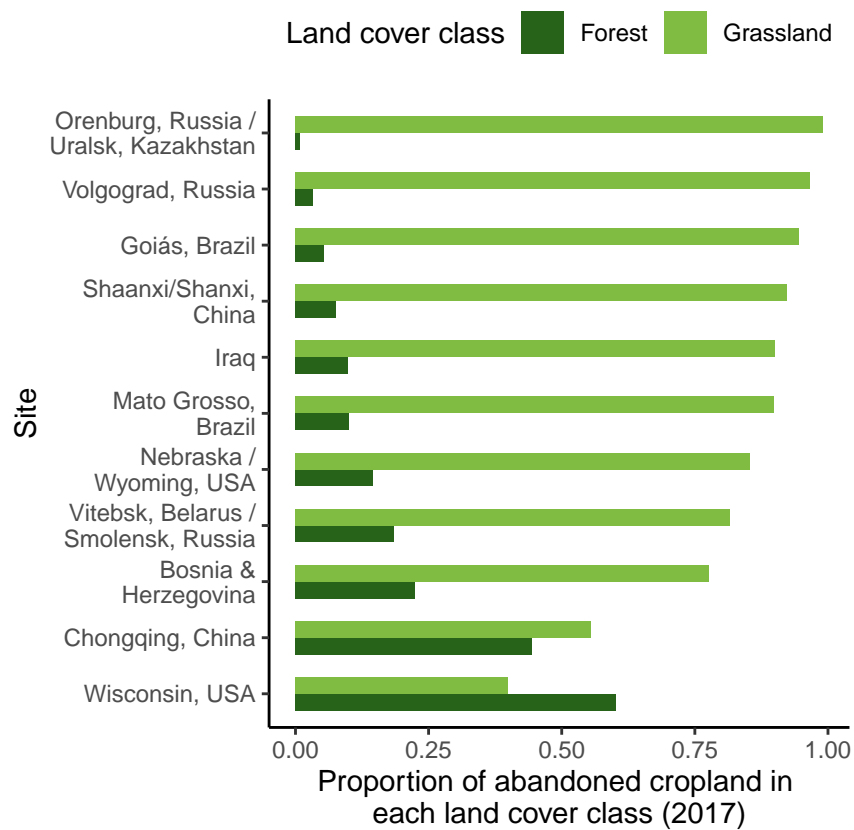


Figure S8: Proportion of abandoned cropland in each land cover class as of 2017.

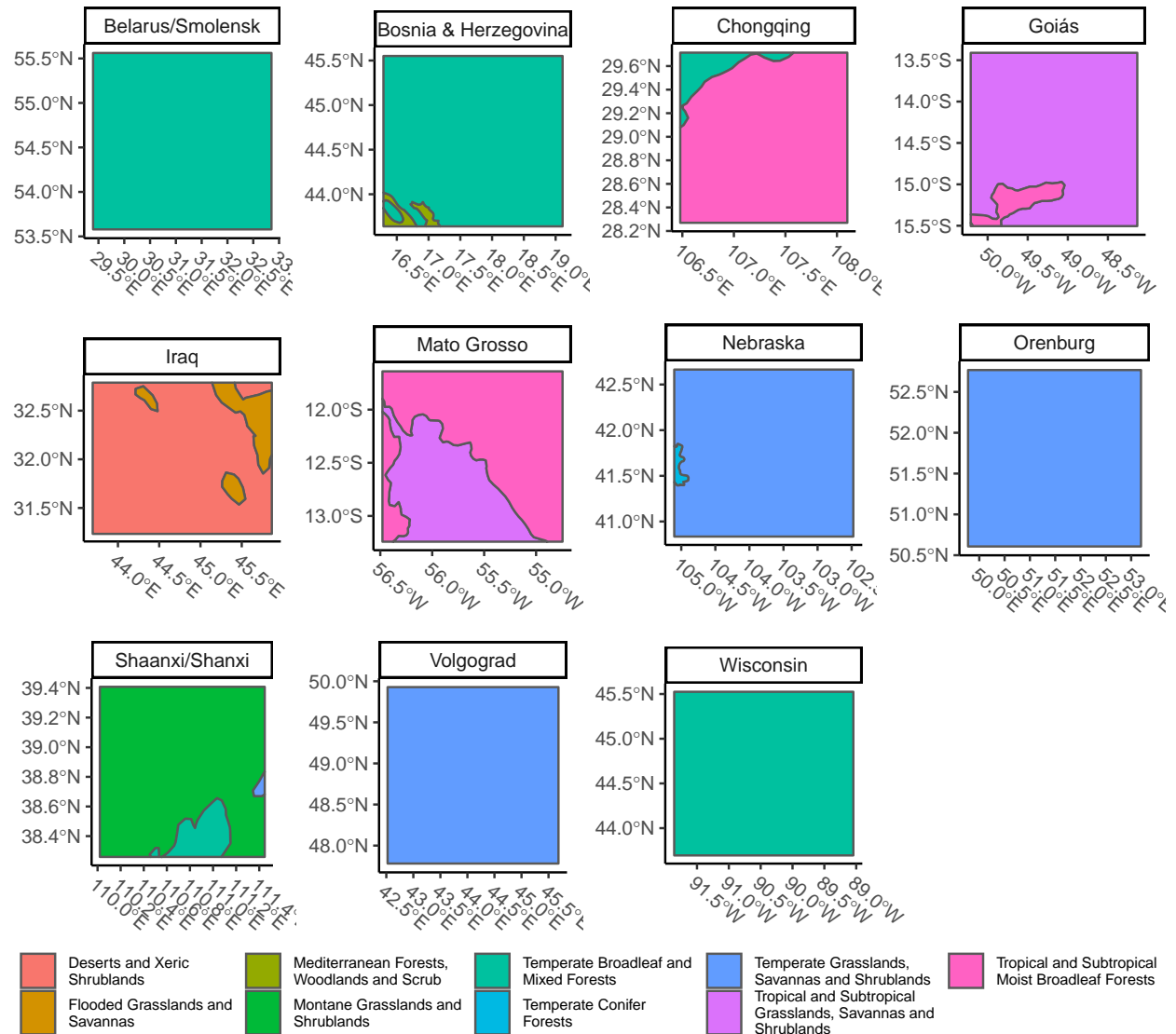


Figure S9: Site biomes, using biome classifications from The Nature Conservancy's Terrestrial Ecoregions of The World (TEOW) database, derived from Olson et al.<sup>12</sup> and Olson and Dinerstein.<sup>13</sup>

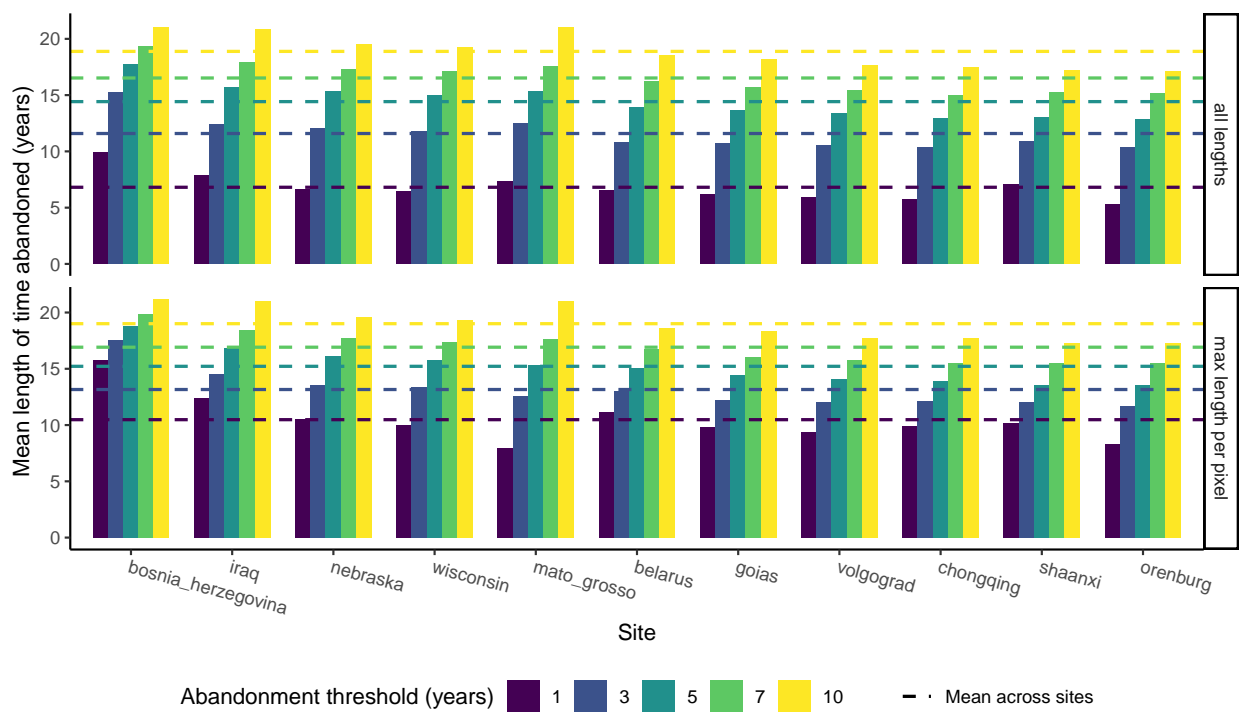


Figure S10: Mean abandonment lengths shown for various abandonment thresholds.

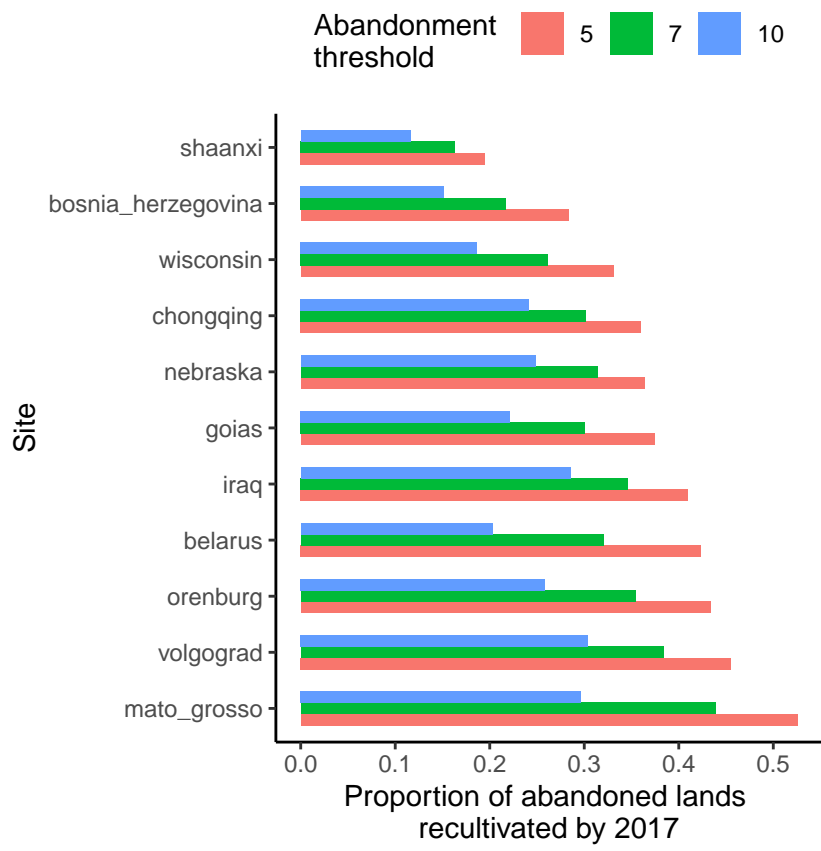


Figure S11: Recultivation rates shown for various abandonment thresholds.

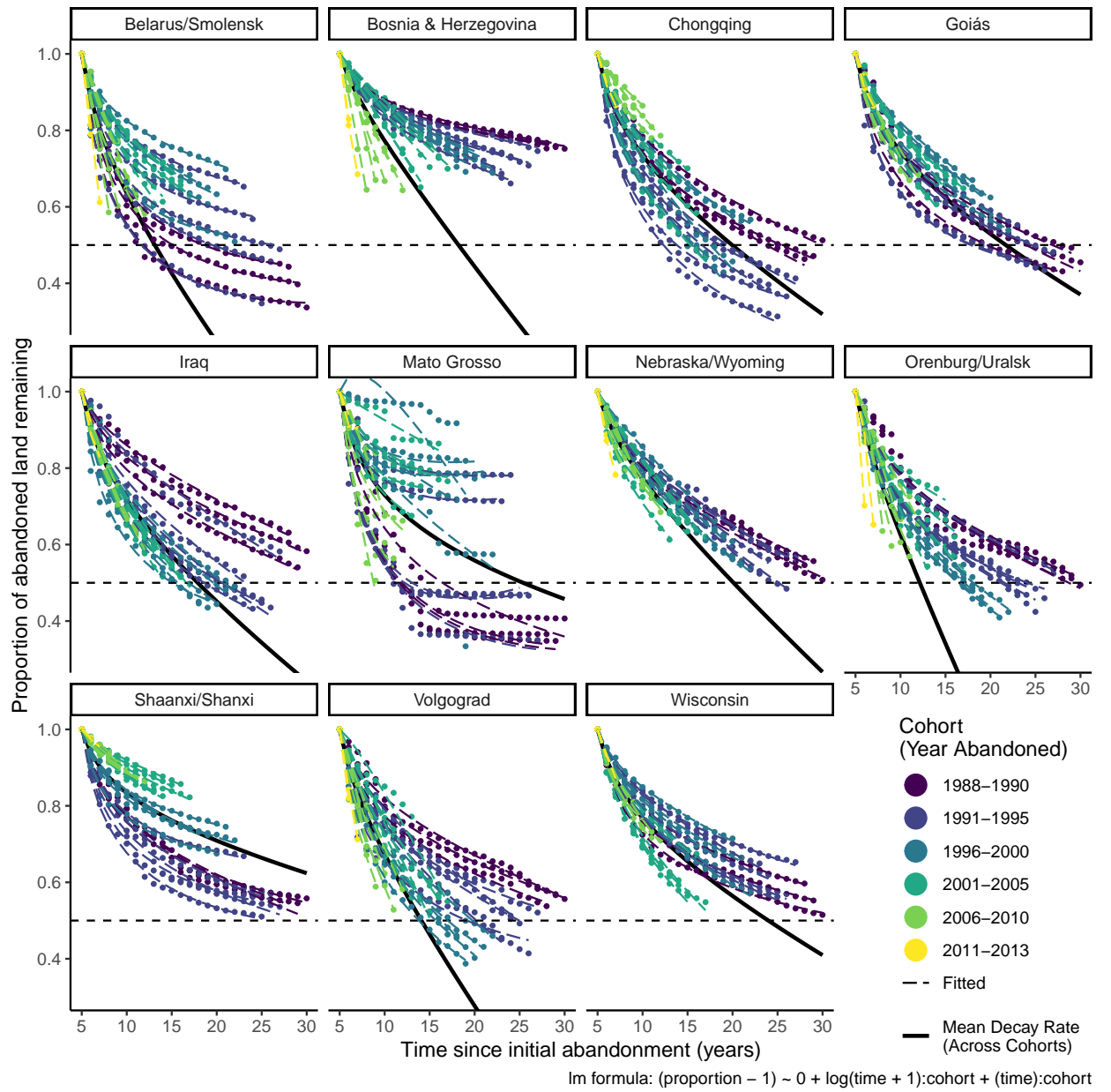


Figure S12: Decay model results for all sites, showing the proportion of each cohort of abandoned land (i.e., all pixels abandoned in a given year) remaining abandoned over time for each of our eleven sites. Points represent actual observations by cohort, dashed lines represent linear model predictions (fitted values) for each cohort as a function of time (including a linear and logarithmic term of time), and the solid black line represents the site-level mean trend across all cohorts (calculated by taking the mean of each time coefficient values across all cohorts, respectively, and using those two mean values to plot a mean trend). Colors of both points and dashed lines correspond to roughly five-year group of cohorts, ranging from dark purple (oldest cohorts) to green and yellow (most recent cohorts). The horizontal black dashed line shows a proportion of 0.5, indicating the point where half of a cohort has been recultivated. Model diagnostic plots are shown in Figures S14 and S15.

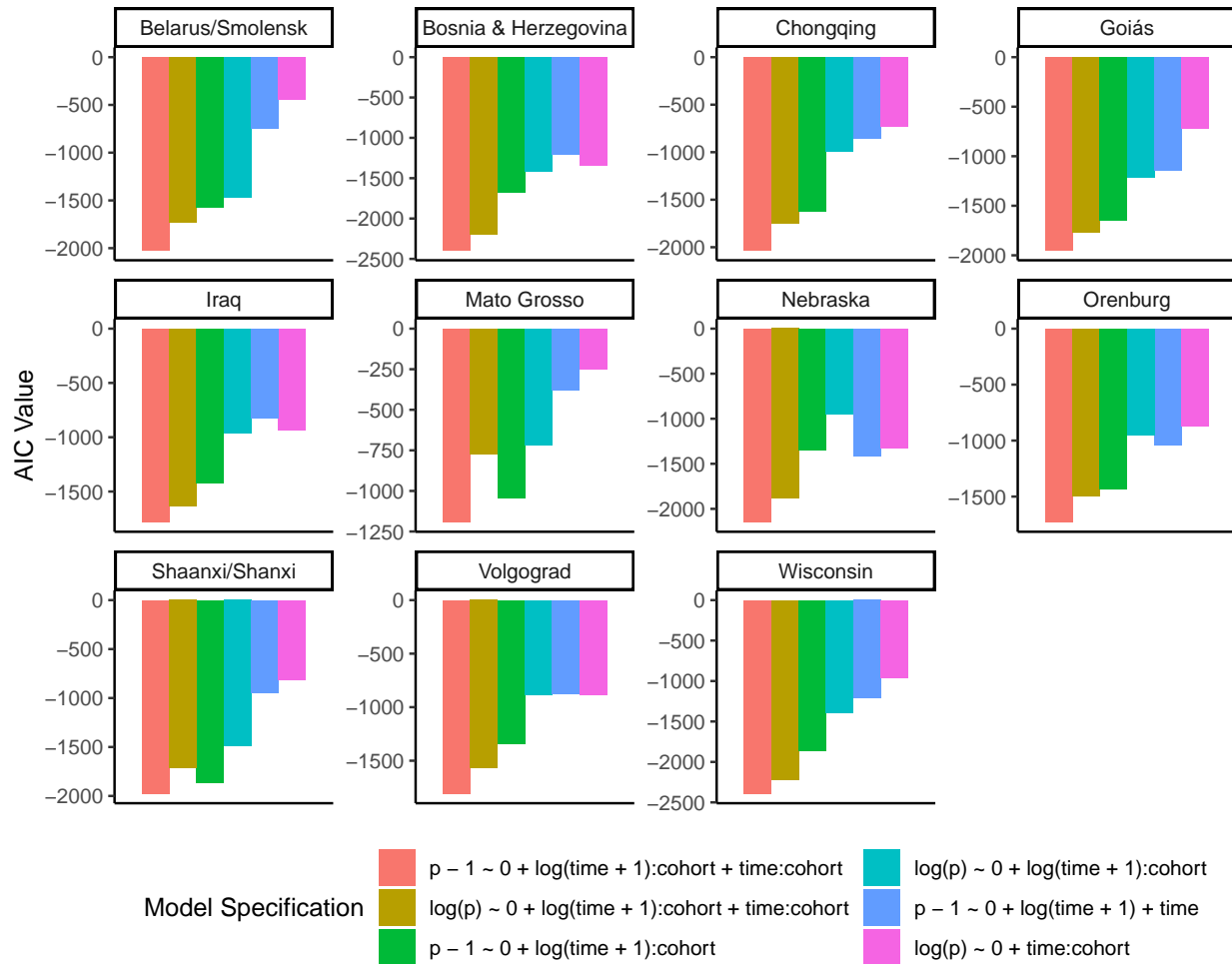


Figure S13: Akaike Information Criterion (AIC) values for various recultivation (“decay”) model specifications for each site. More negative AIC values indicate a better model fit.

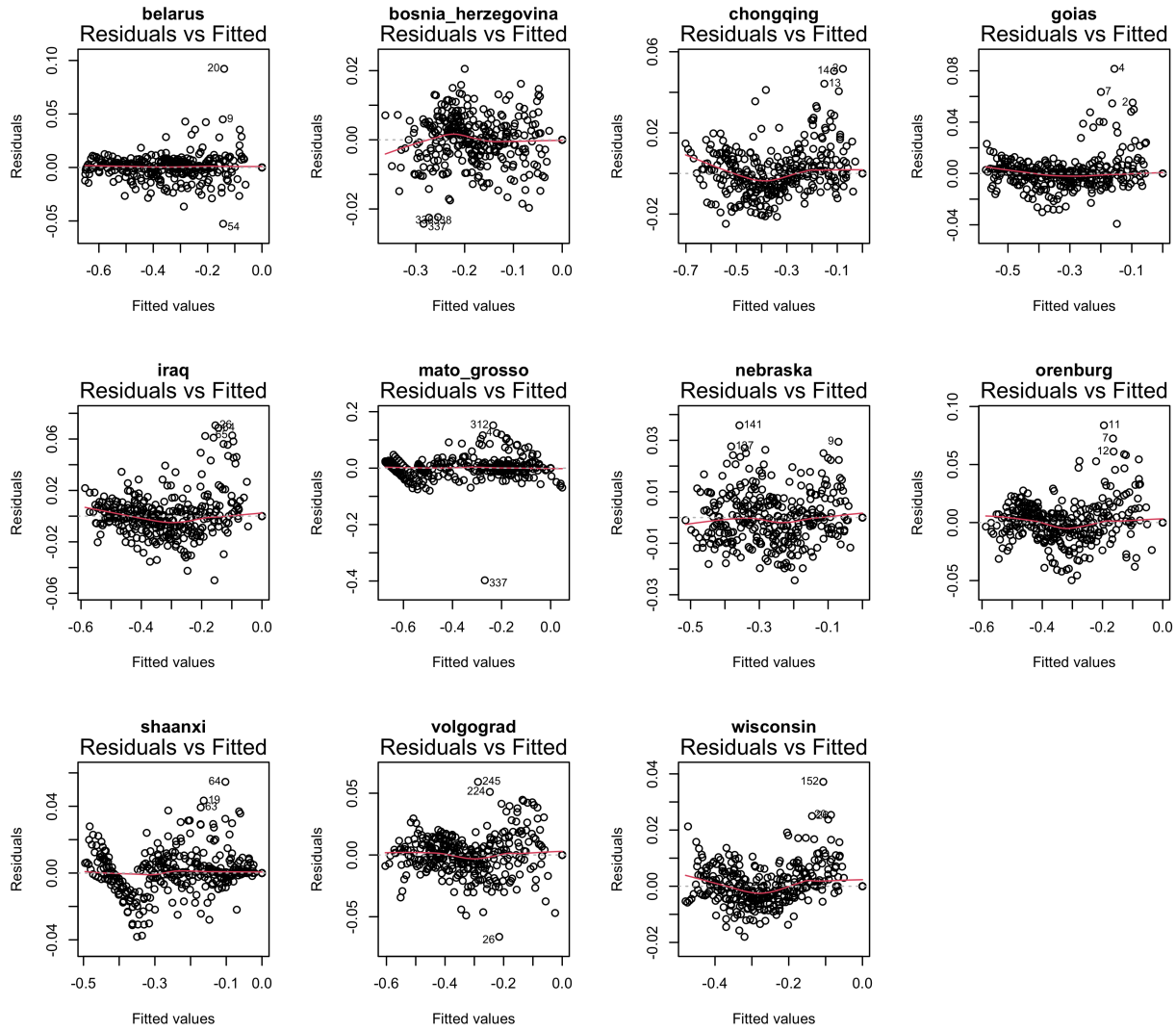


Figure S14: Residuals vs. fitted diagnostic plots for our linear models of the recultivation (“decay”) of abandonment at each site. These models take the form shown in Equation (S2), and are shown in Figure S12.

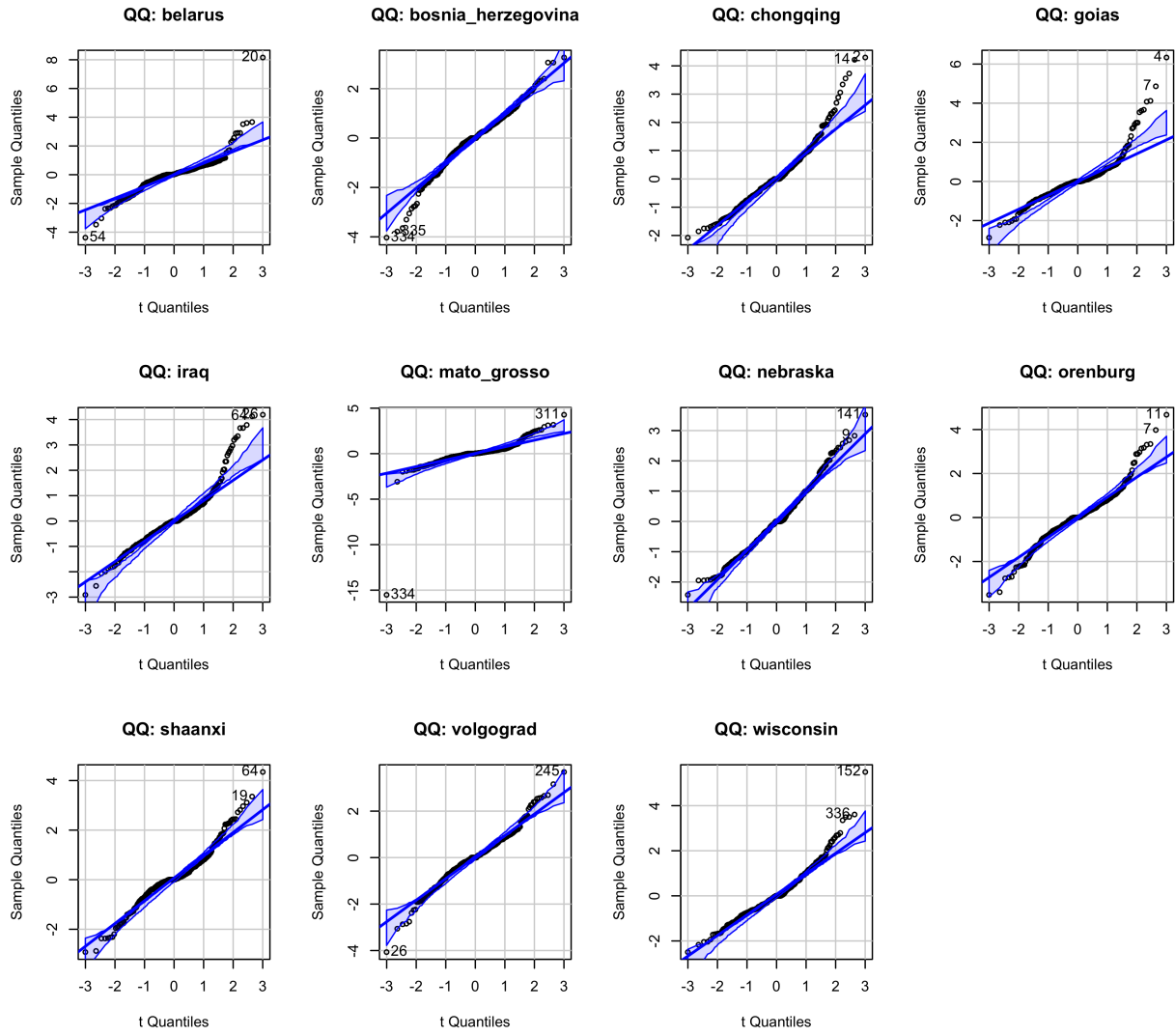


Figure S15: QQ plots calculated using the `{car}` package<sup>14</sup> for our linear models of the recultivation (“decay”) of abandonment at each site. These models take the form shown in Equation (S2), and are shown in Figure S12.

### Mean Decay Rates By Site

Im formula:  $(\text{proportion} - 1) \sim 0 + \log(\text{time} + 1):\text{cohort} + (\text{time}):\text{cohort}$

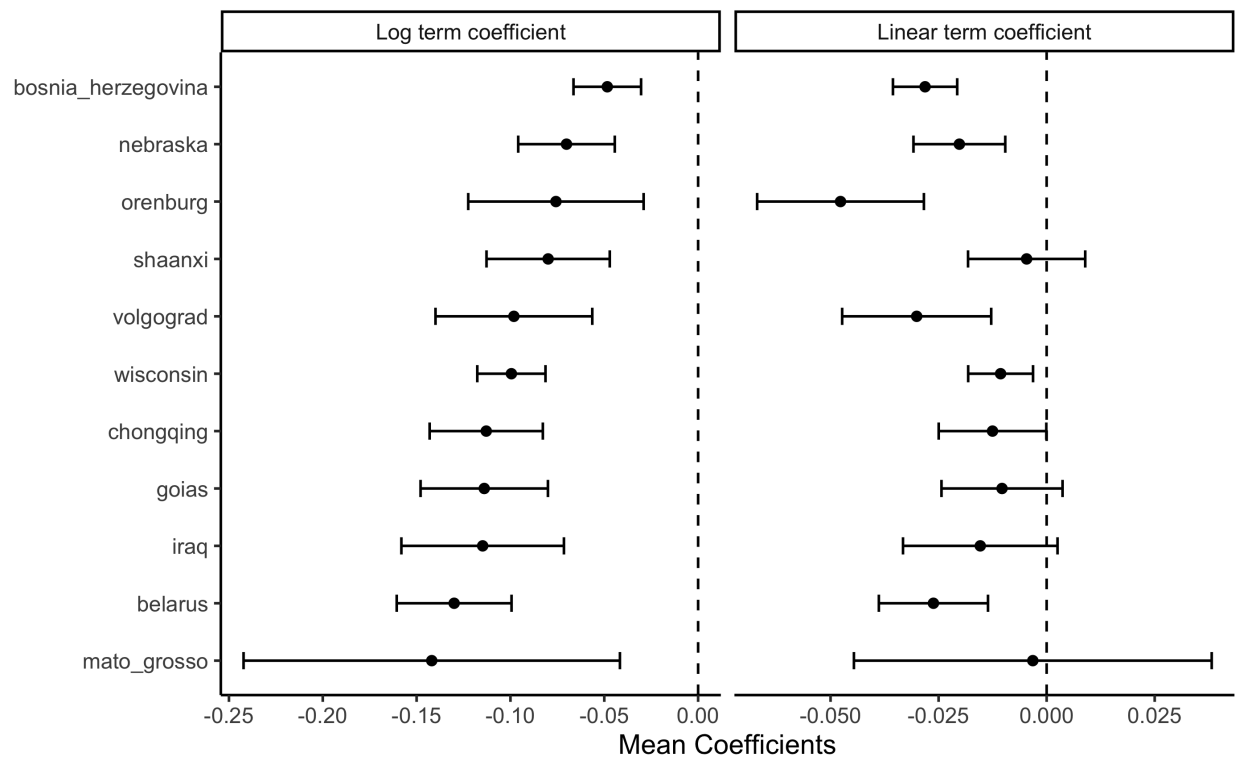


Figure S16: Mean decay model coefficients across cohorts at each site. The left panel shows the mean coefficient on the  $\log(\text{time})$  terms and the right shows the site mean coefficient on the linear time terms. These mean coefficients are used to plot the mean decay trajectories shown in Figure 3.

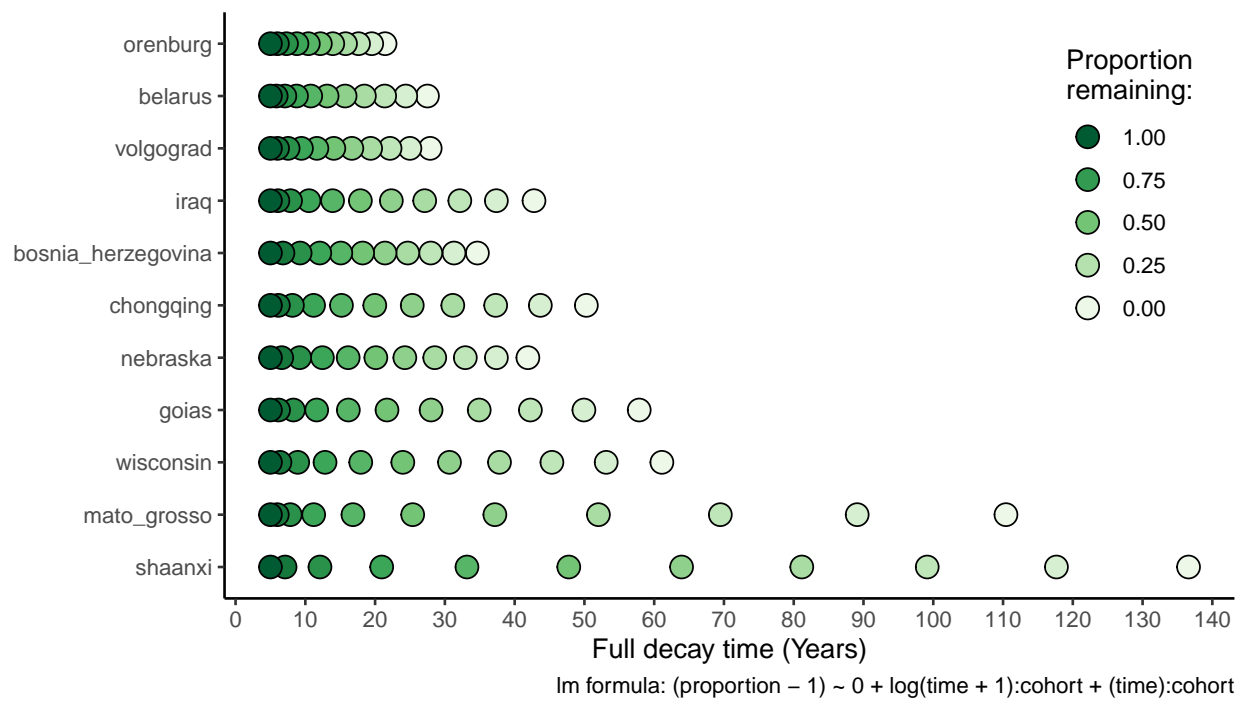


Figure S17: An alternative representation of the mean decay rate for each site (also shown in Figure 3). The color of each point corresponds to the proportion remaining after a given amount of time.

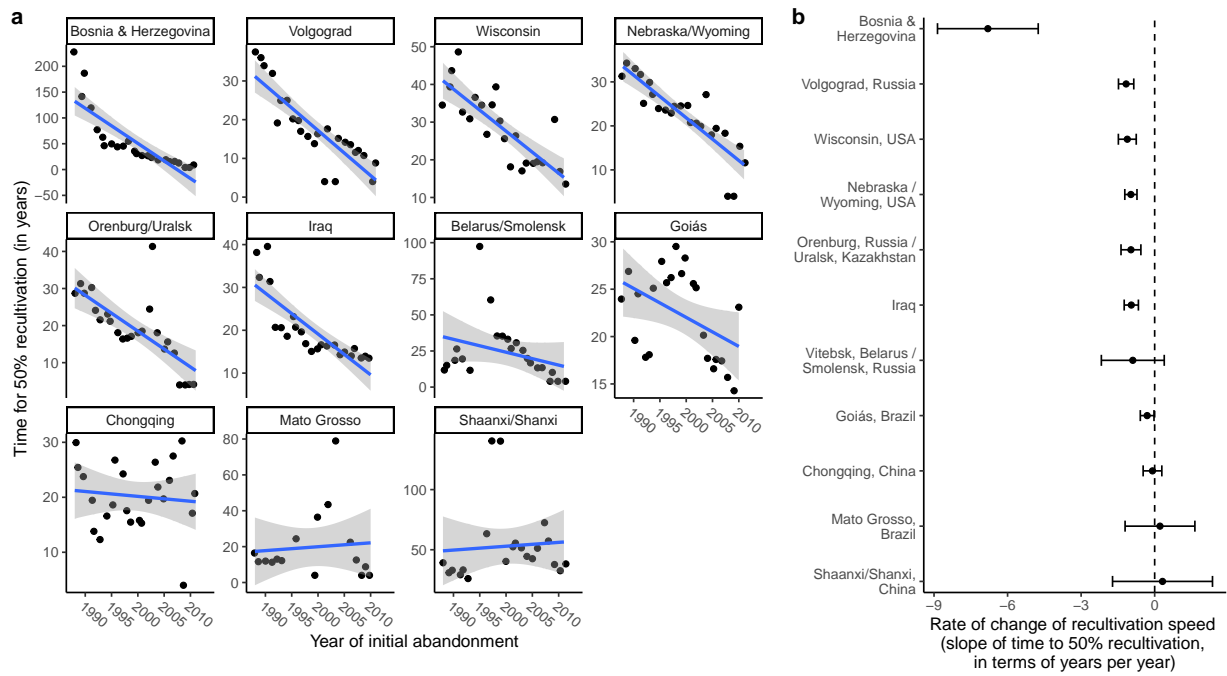


Figure S18: The rate of change of decay rates (measured as the half-life, or the time required for 50% of each cohort to be recultivated) at each site over the course of the time series. Individual site trends are shown in panel a. Solid lines show simple linear regressions, the slopes of which are shown in panel b. Gray bands around the linear trends in panel a and the error bars on slope estimates in panel b both represent 95% confidence intervals. These models are described by Eq. (S3). Model diagnostic plots are shown in Figures S19 and S20.

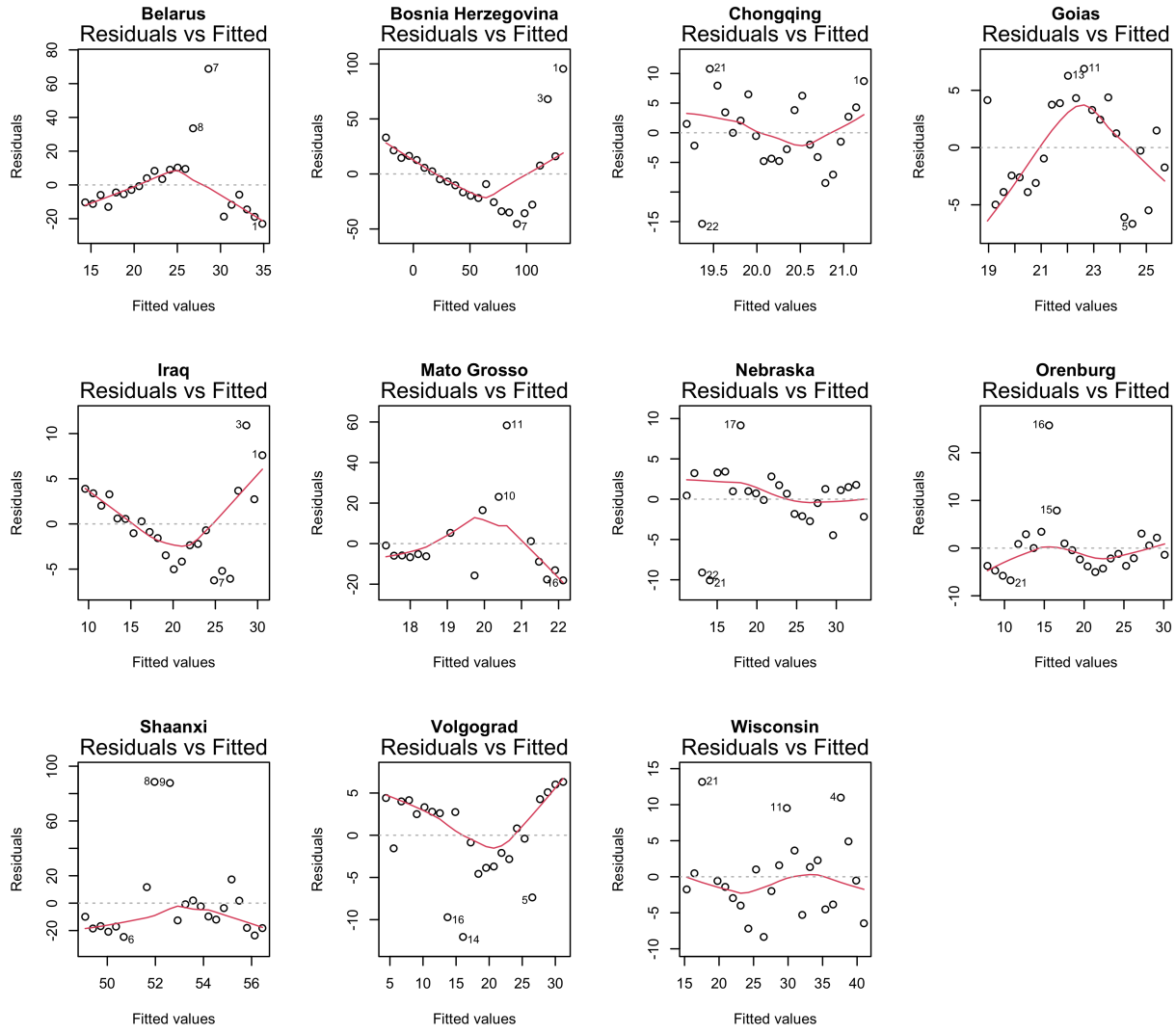


Figure S19: Residuals vs. fitted diagnostic plots for each site, for a simple `lm` call corresponding to Eq. (S3), in which the half-life (i.e., the time required for half (50%) of a given cohort of abandoned cropland to be recultivated) is modeled as a function of the year of initial abandonment at each site.

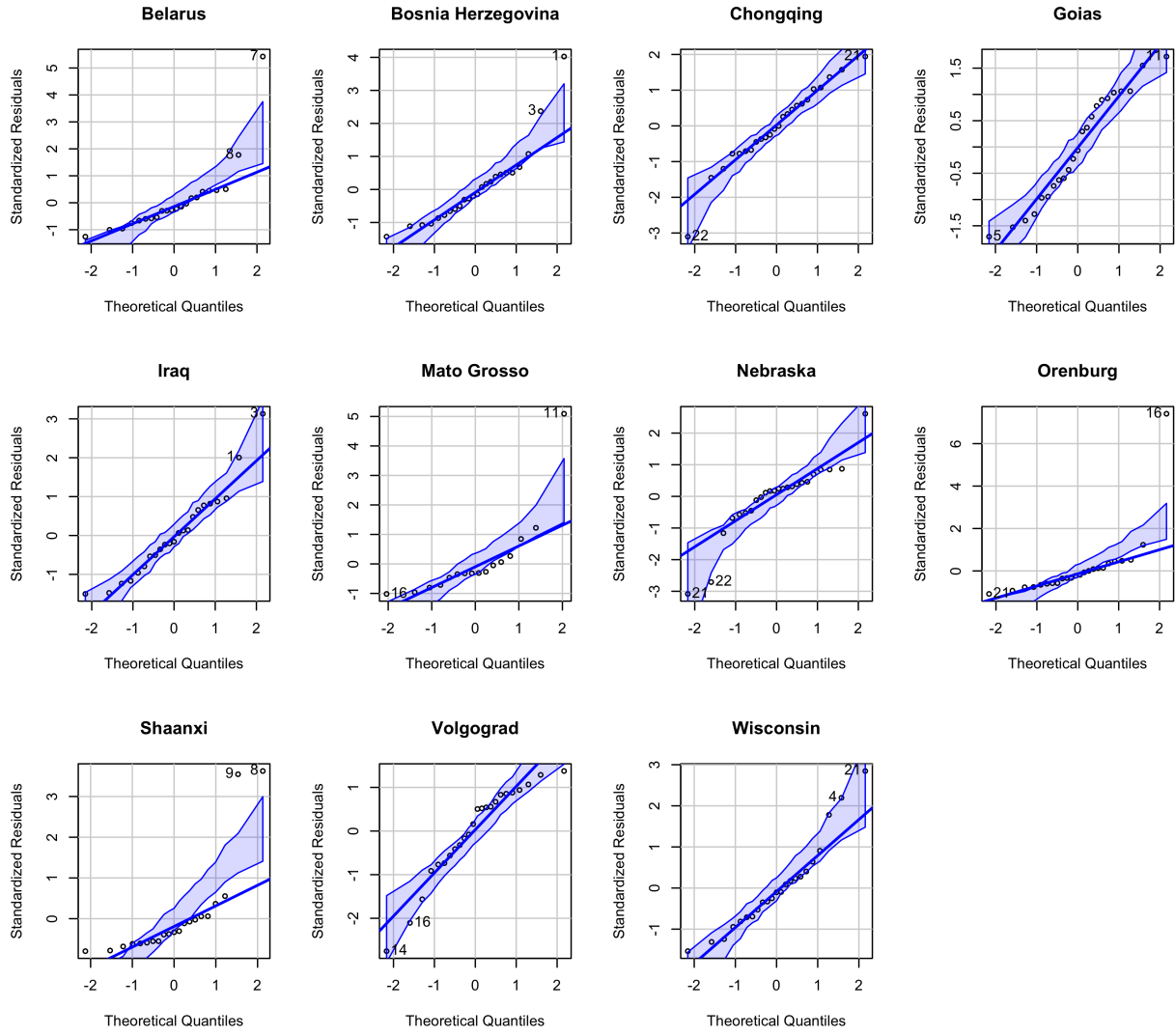


Figure S20: QQ plots calculated using the `car` package (14), for a simple `lm` call corresponding to Eq. (S3), in which the half-life (i.e., the time required for half (50%) of a given cohort of abandoned cropland to be recultivated) is modeled as a function of the year of initial abandonment at each site.

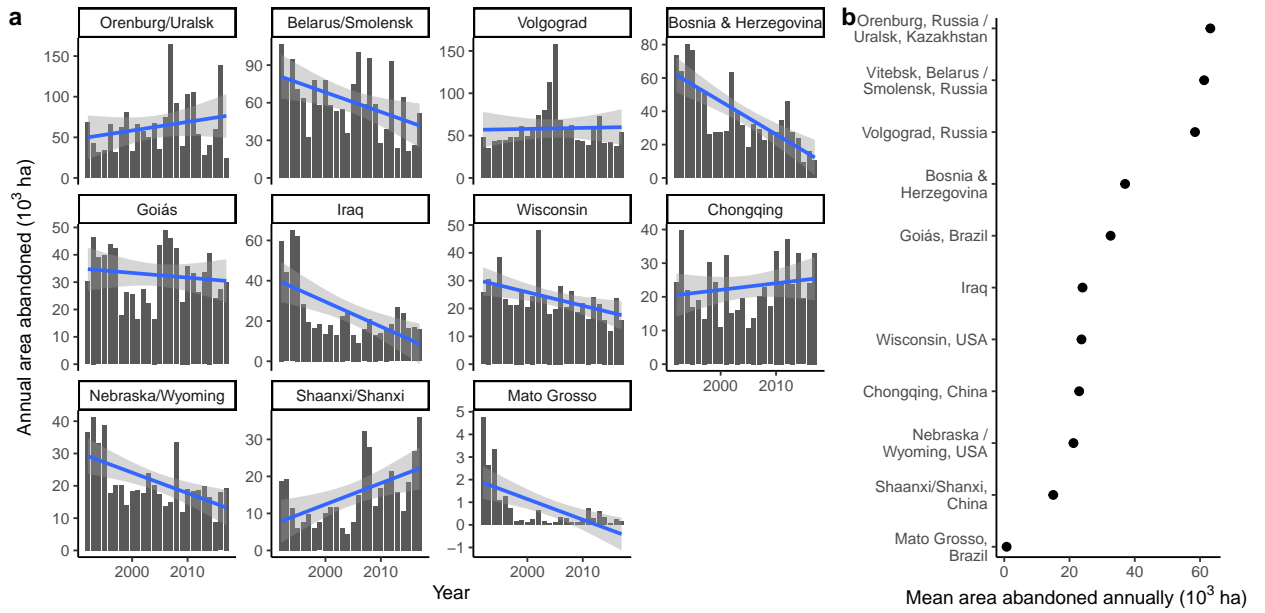


Figure S21: Annual gain in newly abandoned cropland at our eleven sites. Panel a shows the trend in annual abandonment over time at each site (in  $10^3$  ha), and Panel b shows the mean annual abandonment (in  $10^3$  ha) at each site. The mean values in panel b feed into the extrapolations. Note that the annual gain in abandonment corresponds to the dark green bars in Figure S5).

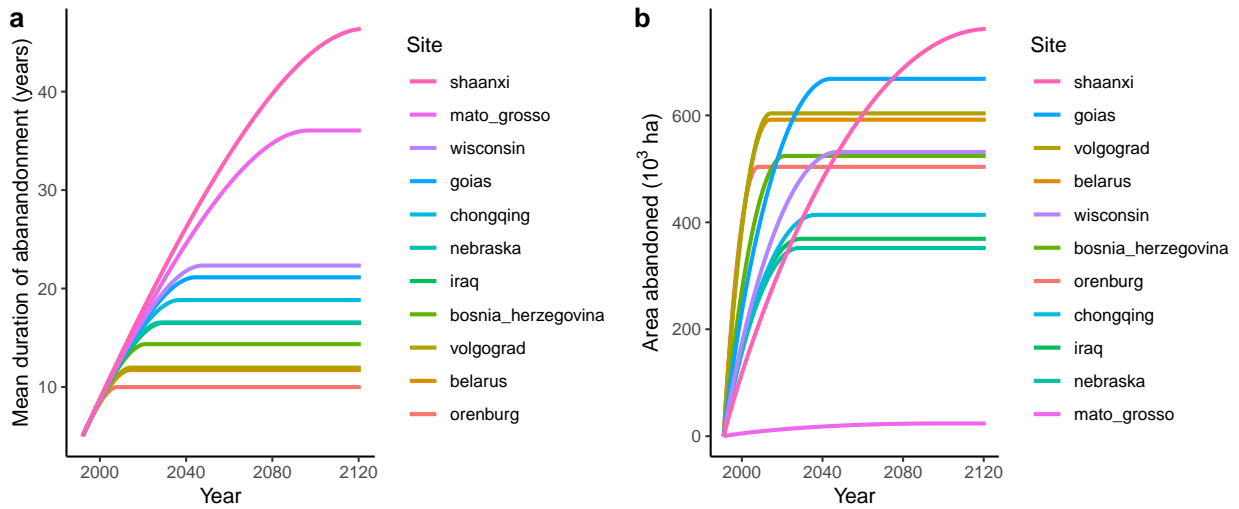


Figure S22: The results of our simple extrapolation, including a) the mean age of abandonment, and b) the total area abandoned into the future. Colors corresponding to each site are consistent across the three panels. These extrapolations assume recultivation based on the mean decay trend for each site Figure 3 and annual new abandonment based on the mean annual gain in abandonment shown in Figure S5 (dark green bars).

## Extrapolation 1

Assuming i) mean decay rates and ii) constant area abandoned each year.

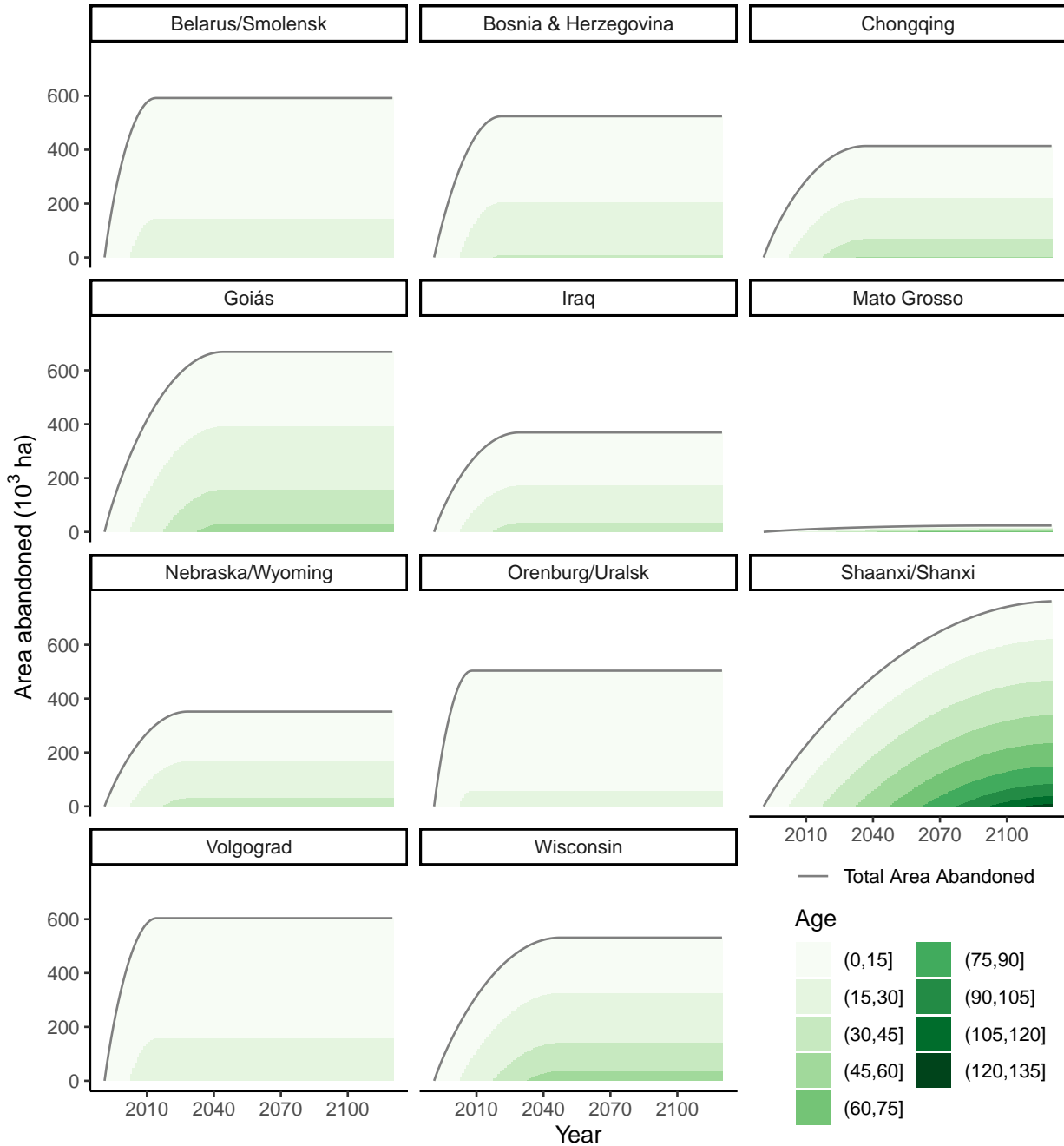


Figure S23: Extrapolating area by age bin, assuming a 1) each site follows the mean recultivation (“decay”) rate, and 2) a constant area abandoned each year (based on the mean annual area abandoned at each site).

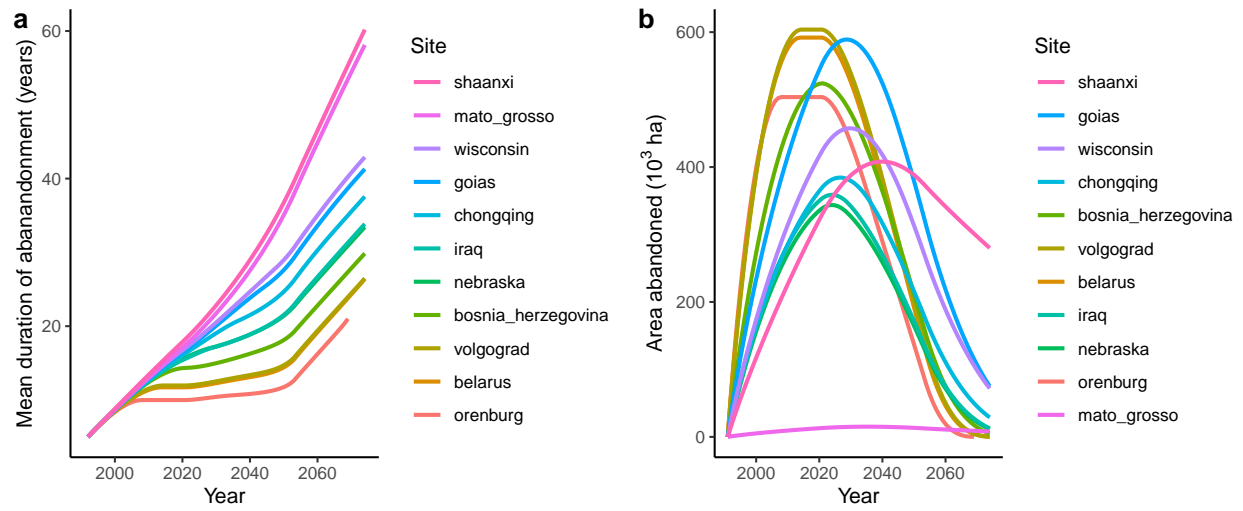


Figure S24: The results of our second extrapolation, including a) the mean age of abandonment, and b) the total area abandoned into the future. Colors corresponding to each site are consistent across the three panels. These extrapolations assume recultivation based on the mean decay trend for each site (Figure 3) and annual new abandonment based on the mean annual gain in abandonment shown in Figure S5 (dark green bars).

## Extrapolation 2

Assuming i) mean decay rates and ii) constant area abandoned each year until 2017, then linear decline in area abandoned each year until reaching 0 in 2050.

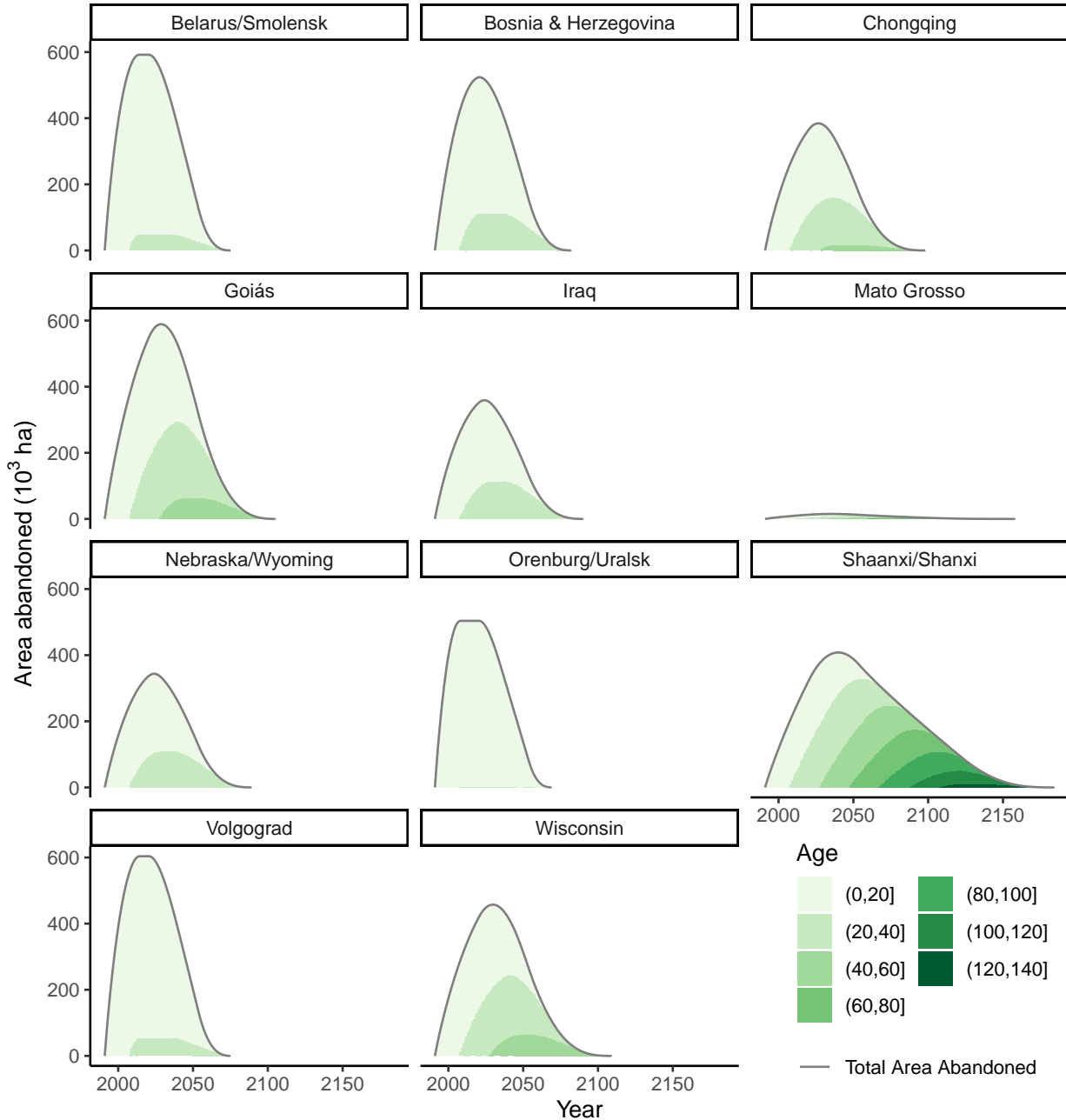


Figure S25: Extrapolating area by age bin, assuming a 1) each site follows the mean recultivation (“decay”) rate, and 2) a constant area abandoned each year until 2017 (based on the mean annual area abandoned at each site), followed by a linearly declining area abandoned each year until reaching 0 in 2050.

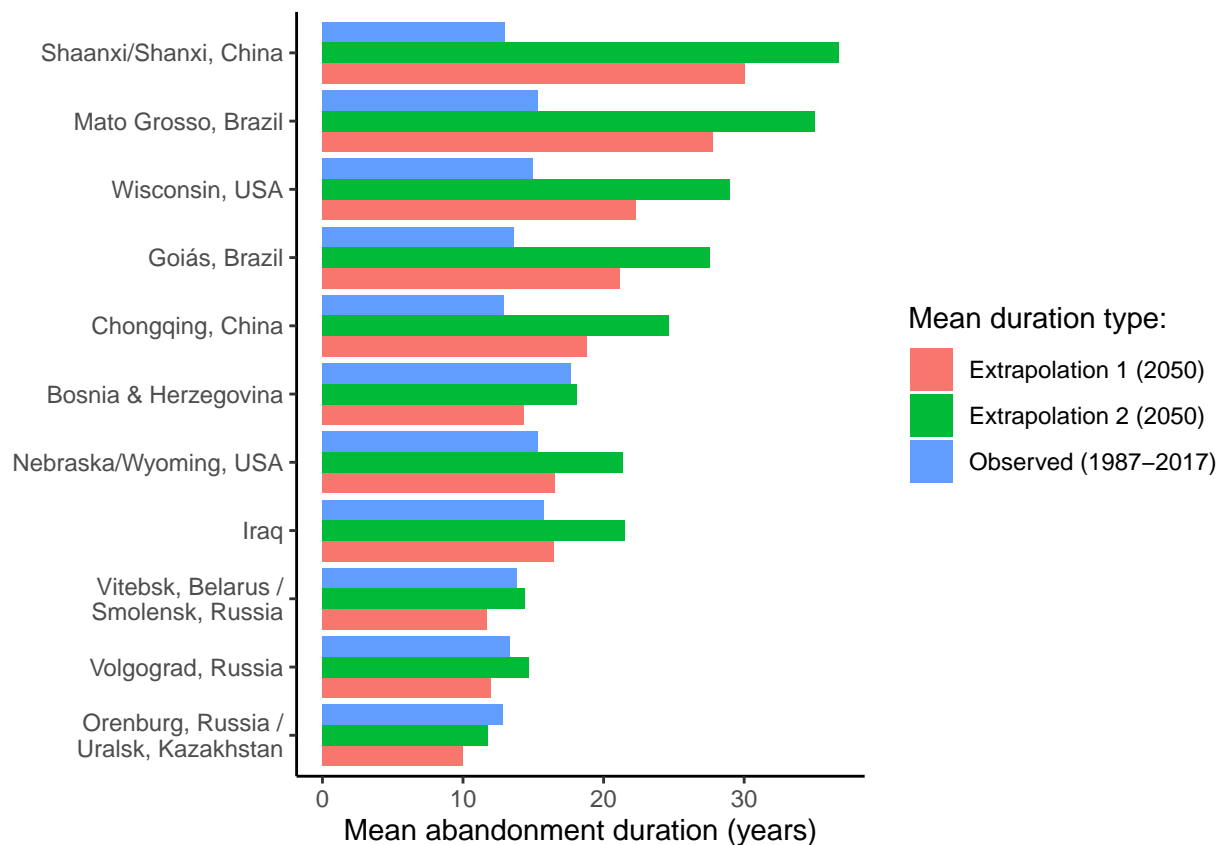


Figure S26: Comparing the mean duration of abandonment at our 11 sites observed between 1987 and 2017 with the extrapolated mean duration as of 2050 for our two extrapolations.

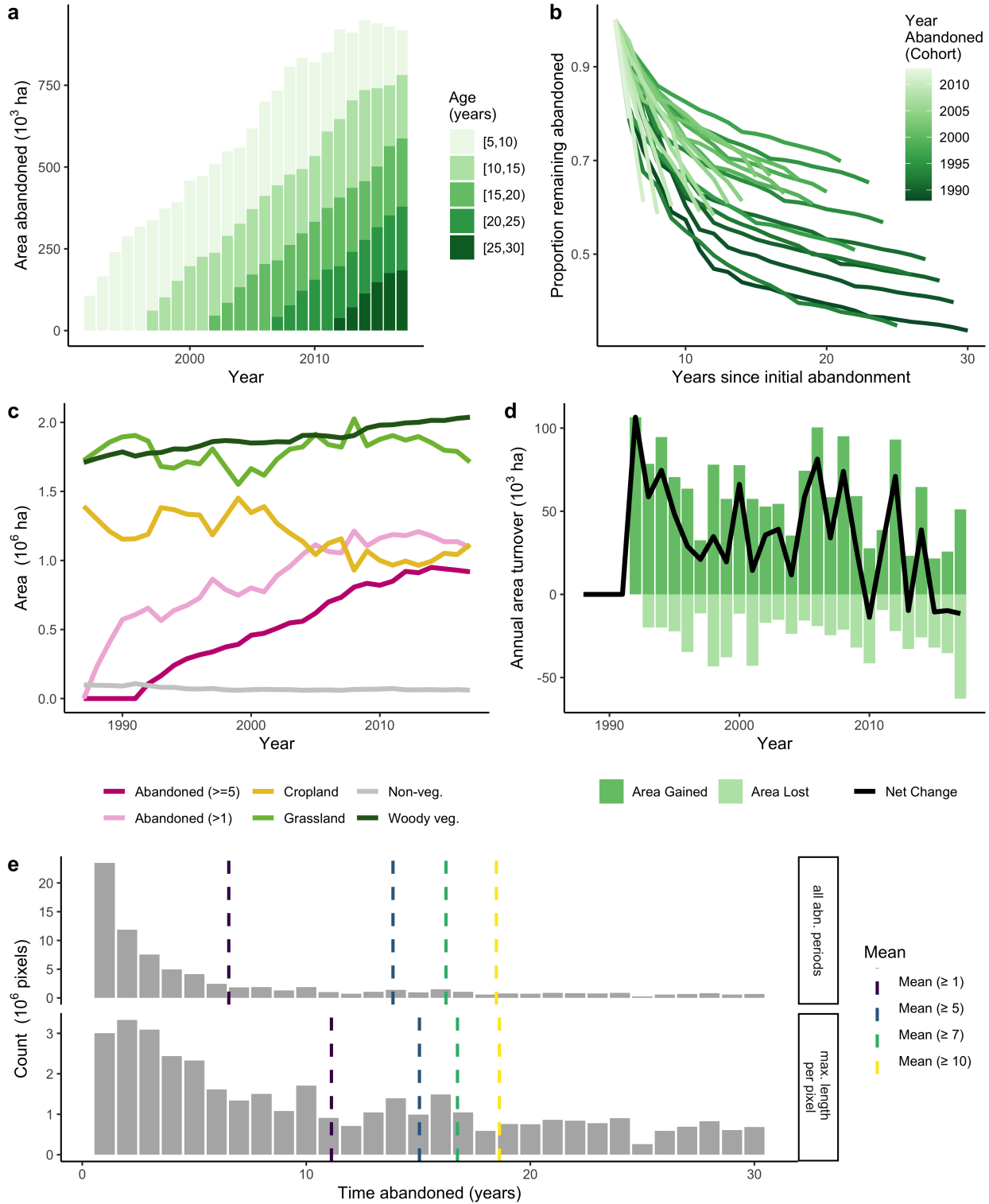


Figure S27: Abandonment patterns for Vitebsk, Belarus / Smolensk, Russia, showing a) accumulation of abandoned land by age class, b) decay of abandoned land by year abandoned, c) the area in each land cover class through time (including both land that has been abandoned for five or more years, as well as any land abandoned for 1 or more years, therefore including short-term fallows), d) the annual turnover of abandoned land through time, and e) the distribution of abandonment duration for all periods of cropland abandonment (top) and the maximum duration of abandonment at each pixel (bottom).

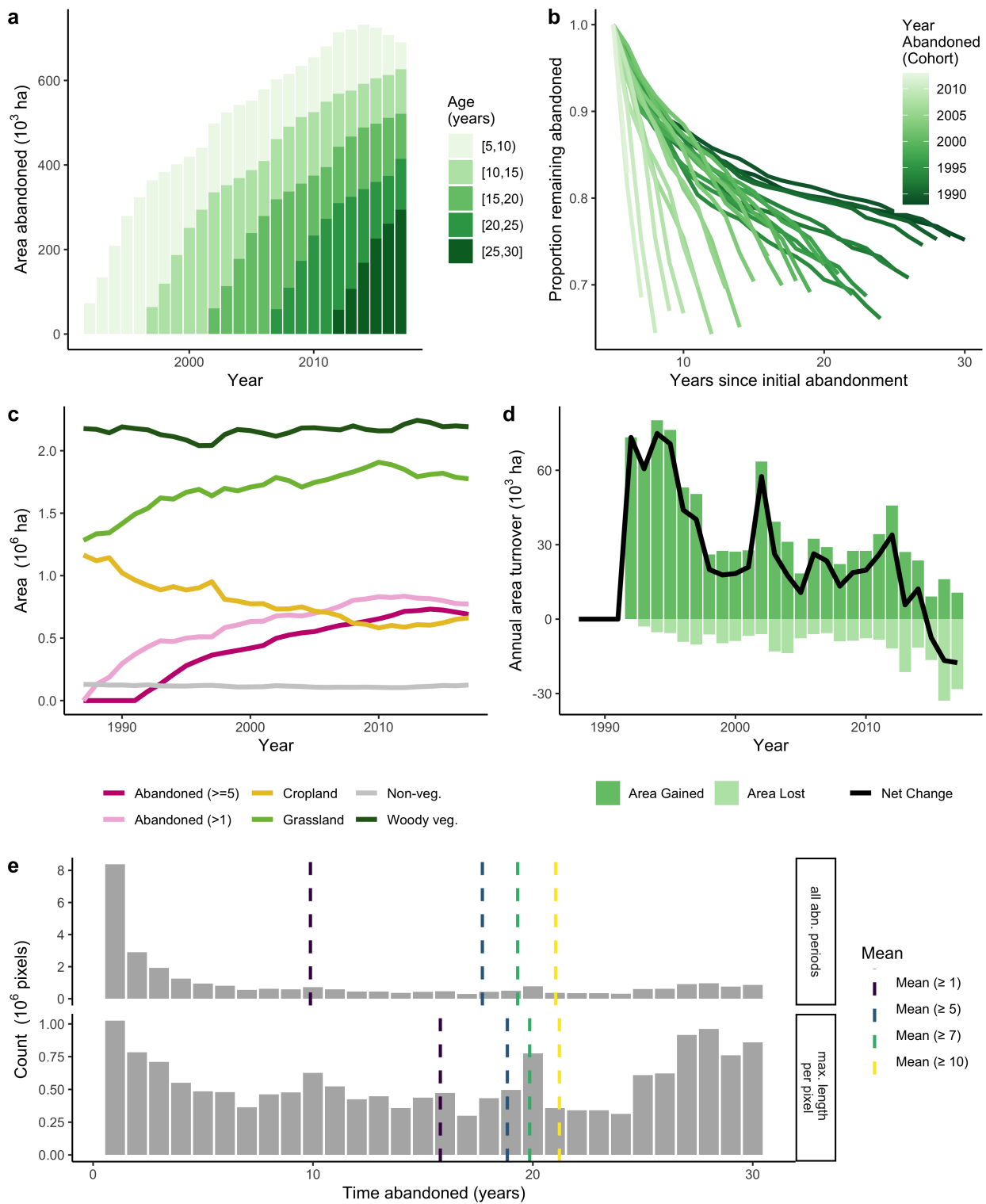


Figure S28: Abandonment patterns for Bosnia & Herzegovina, following Figure S27.

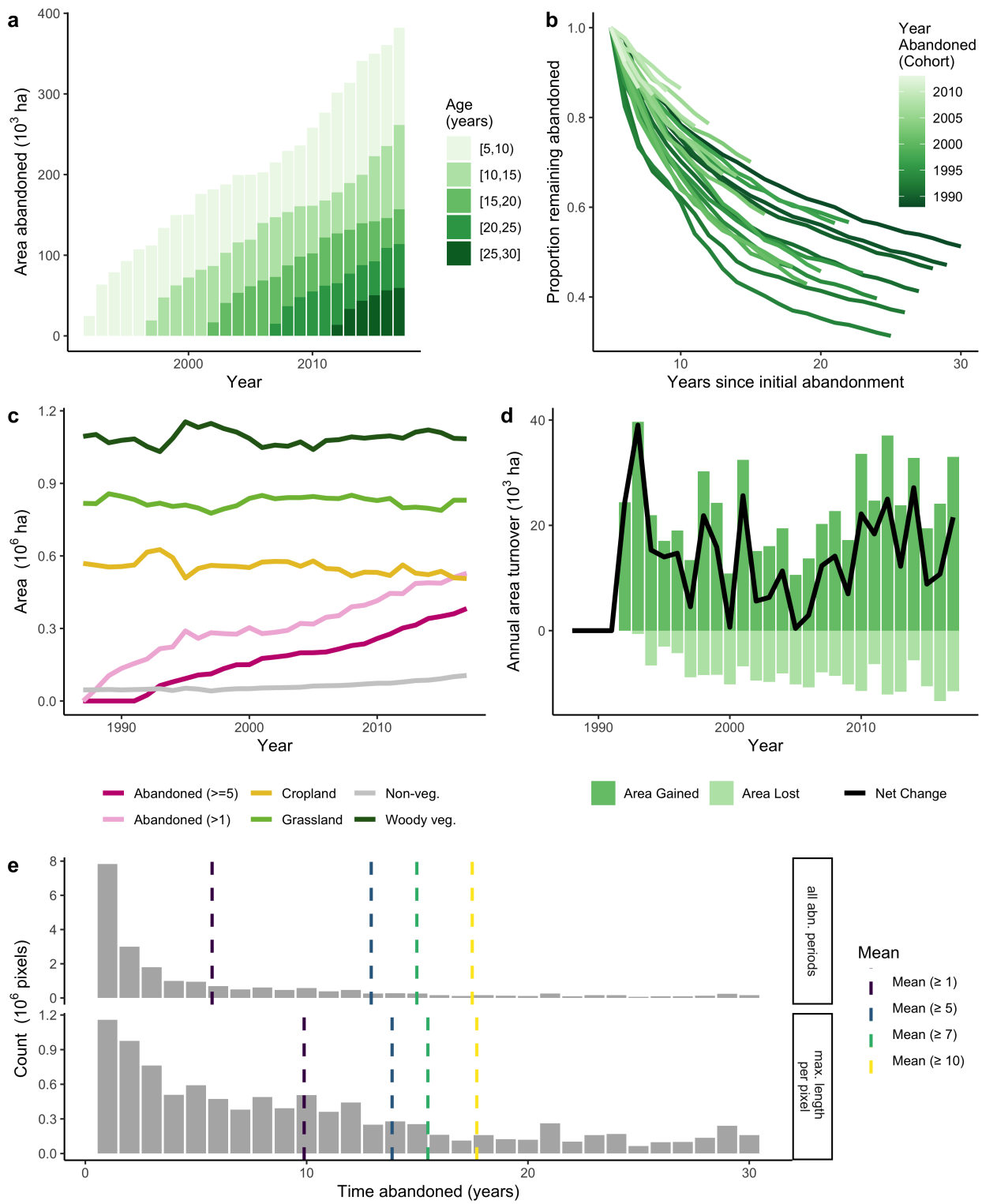


Figure S29: Abandonment patterns for Chongqing, China, following Figure S27.

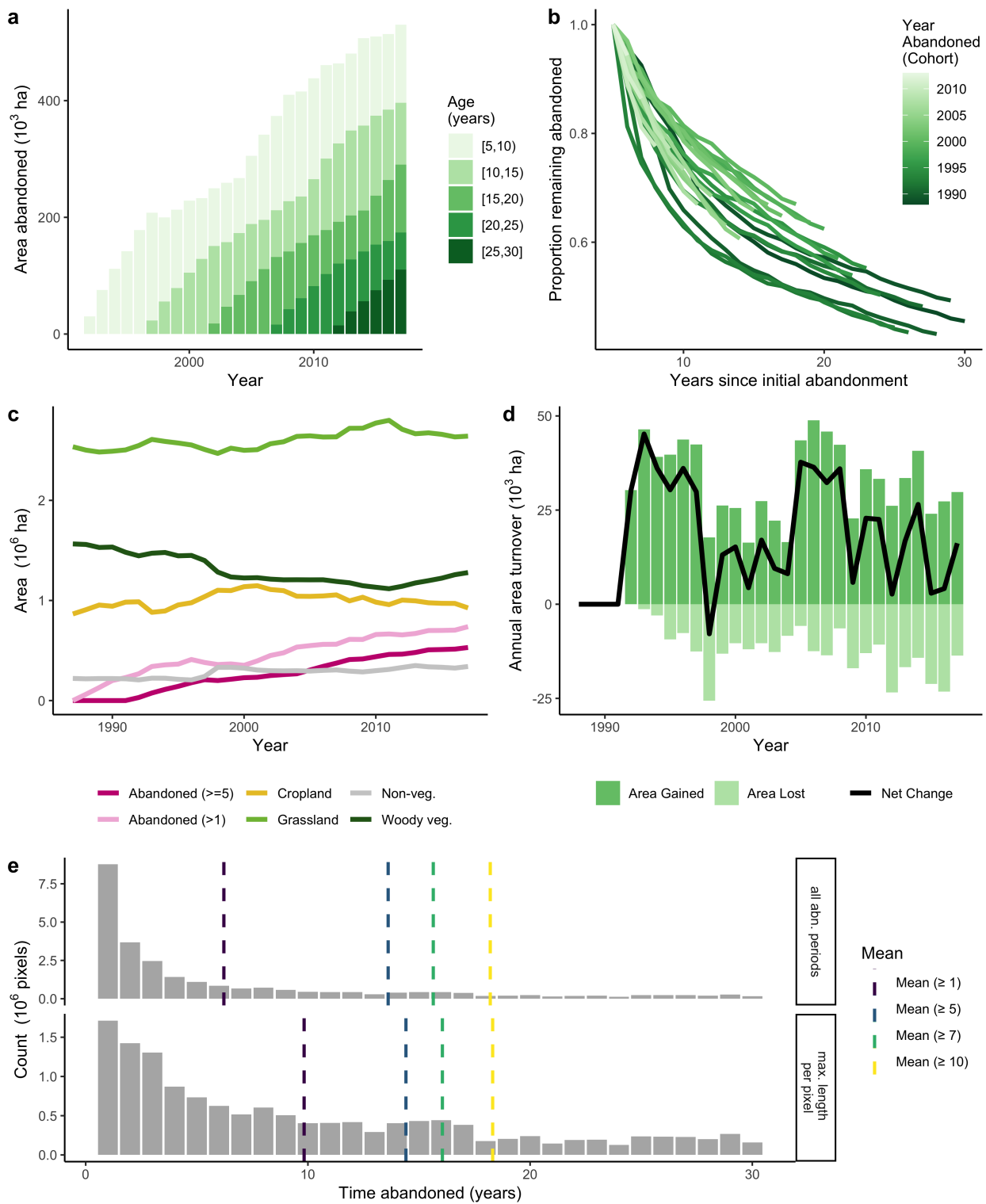


Figure S30: Abandonment patterns for Goiás, Brazil, following Figure S27.

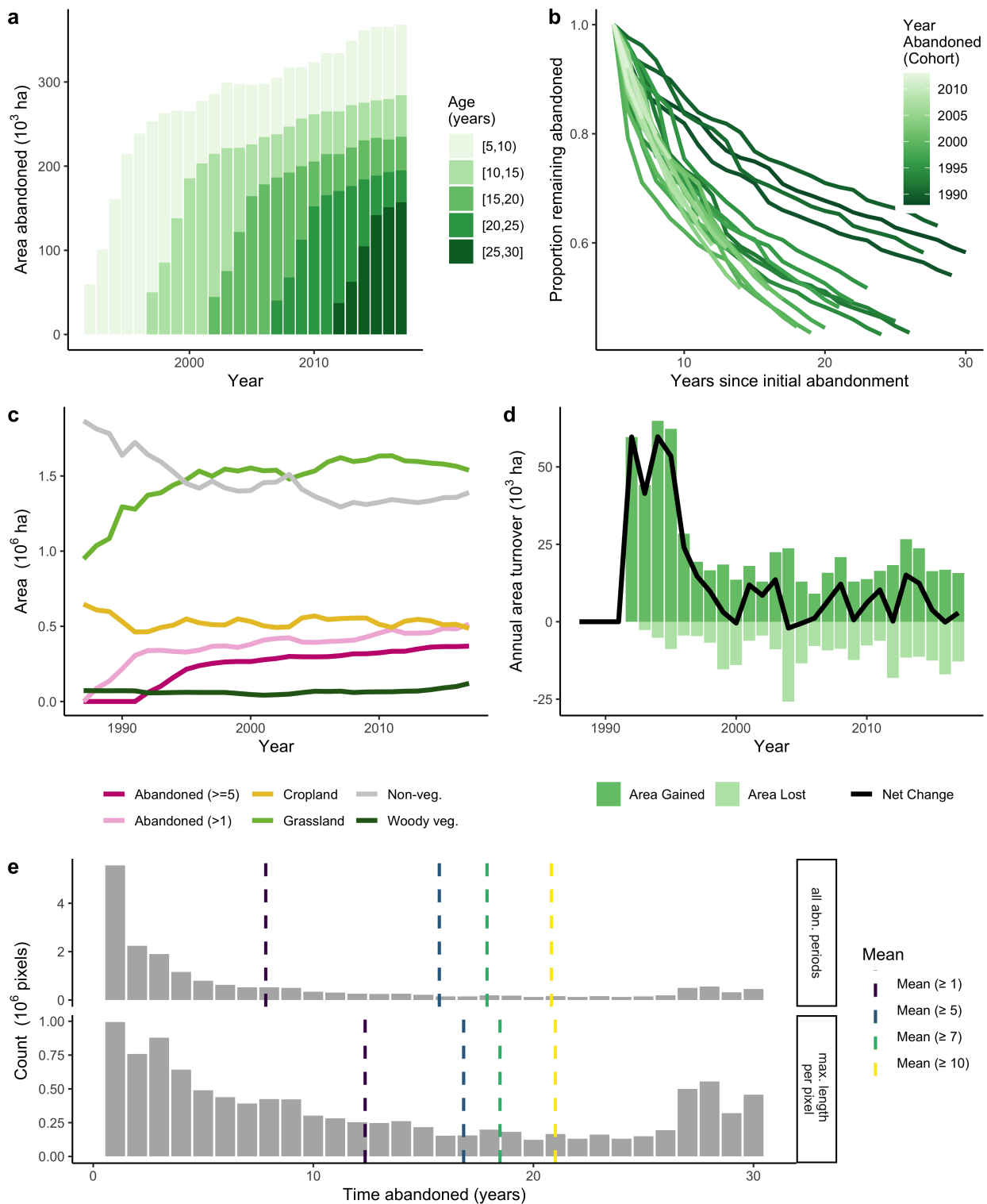


Figure S31: Abandonment patterns for Iraq, following Figure S27.

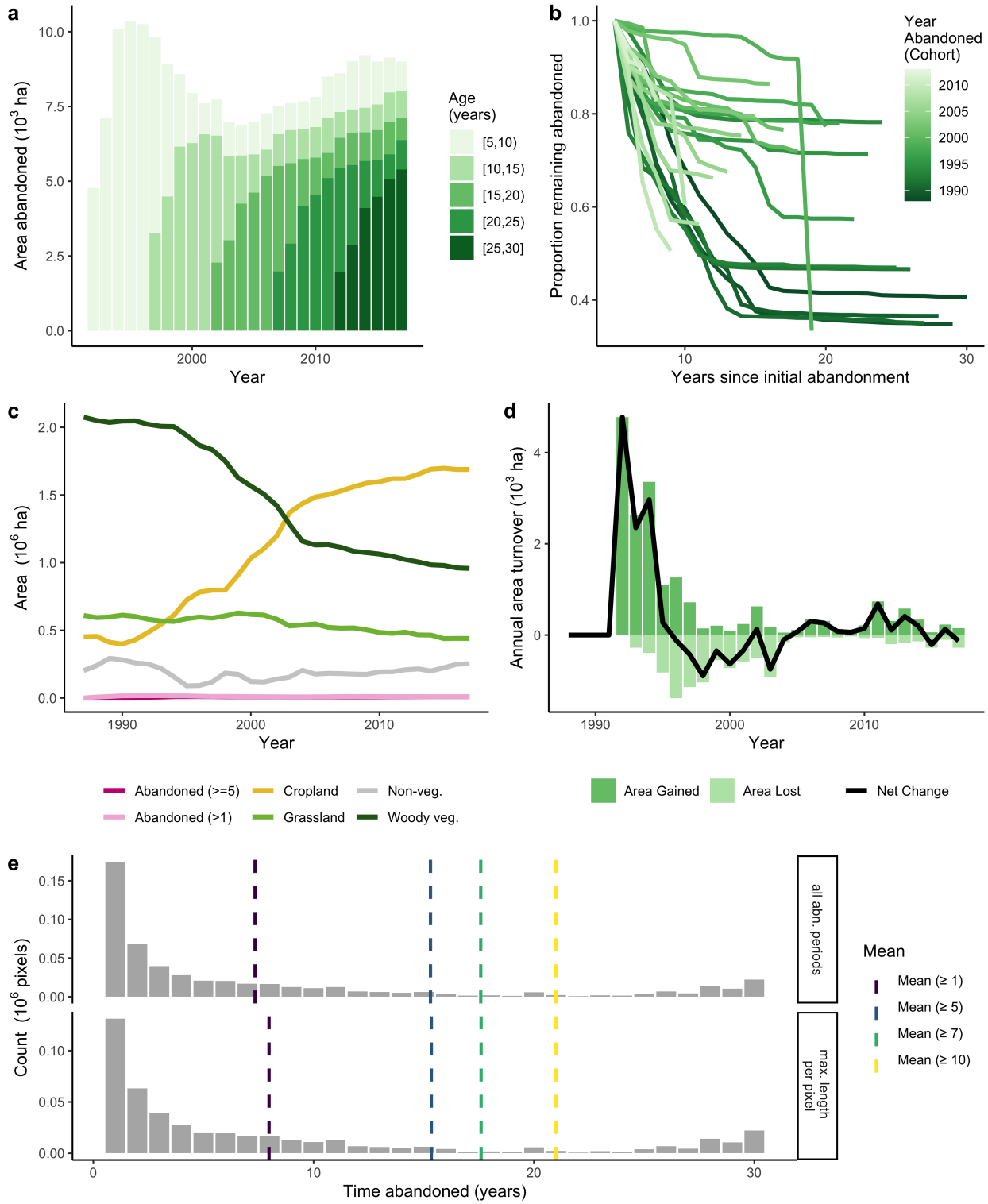


Figure S32: Abandonment patterns for Mato Grosso, Brazil, following Figure S27.

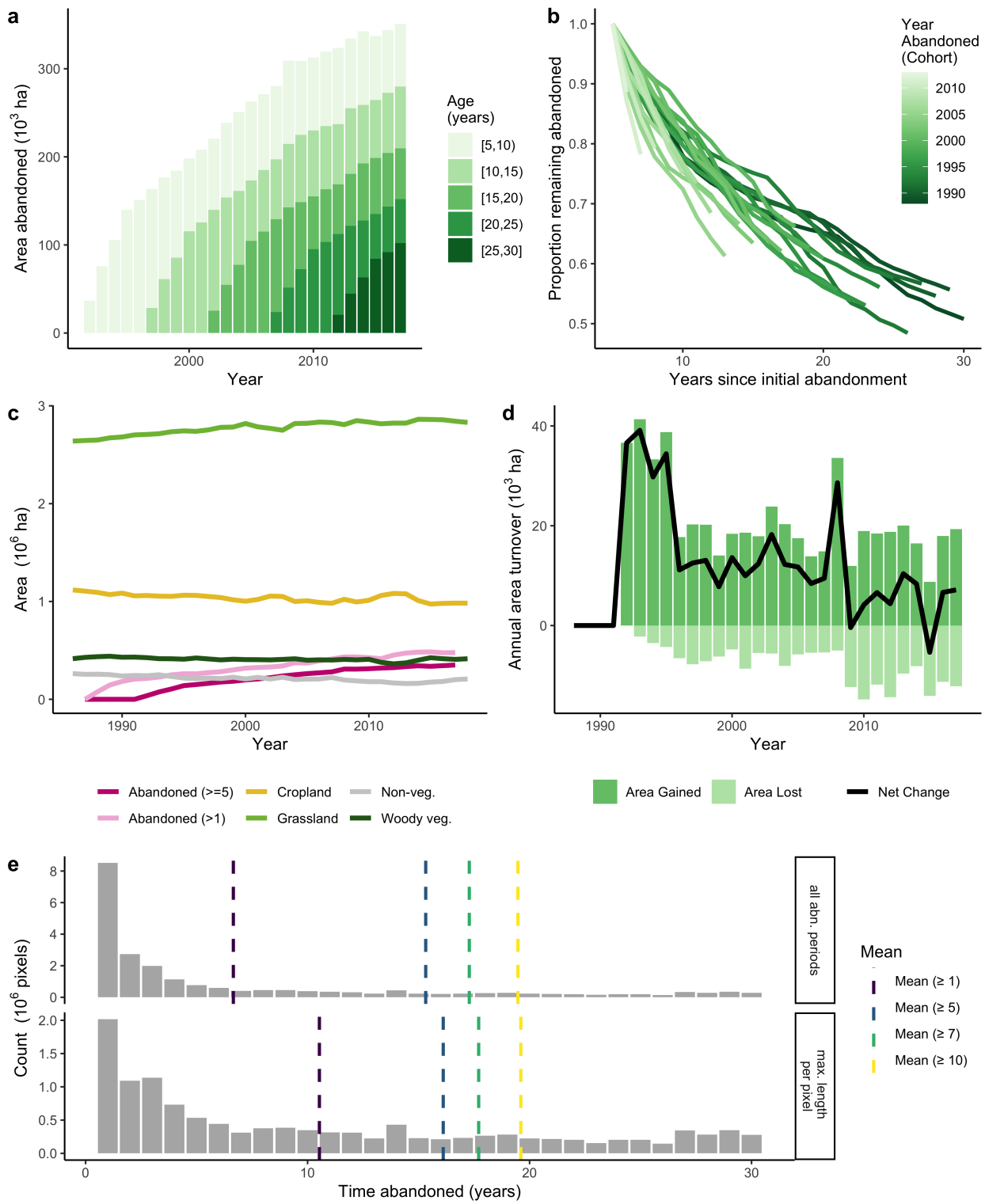


Figure S33: Abandonment patterns for Nebraska/Wyoming, USA, following Figure S27.

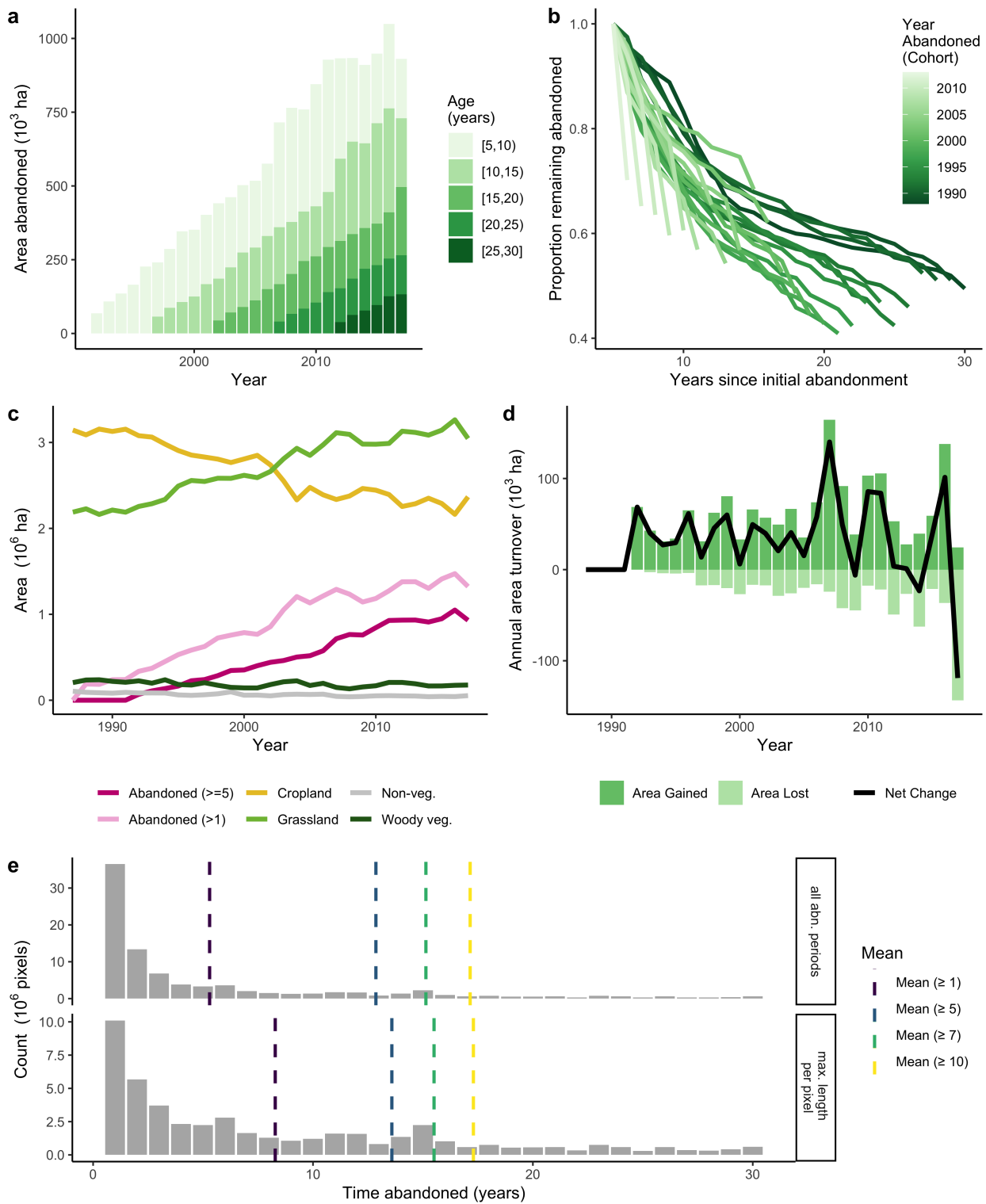


Figure S34: Abandonment patterns for Orenburg, Russia / Uralsk, Kazakhstan, following Figure S27.

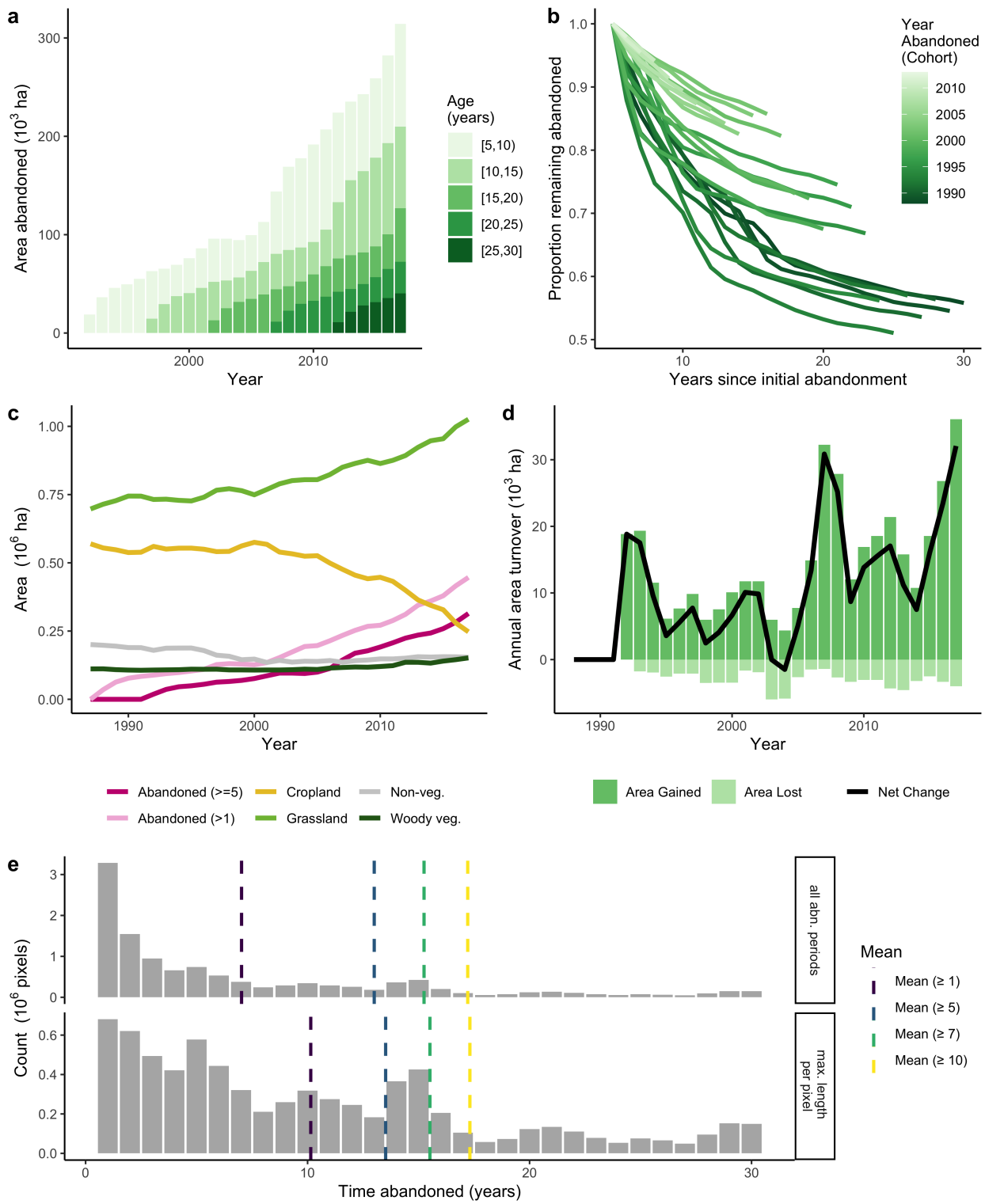


Figure S35: Abandonment patterns for Shaanxi/Shanxi, China, following Figure S27.

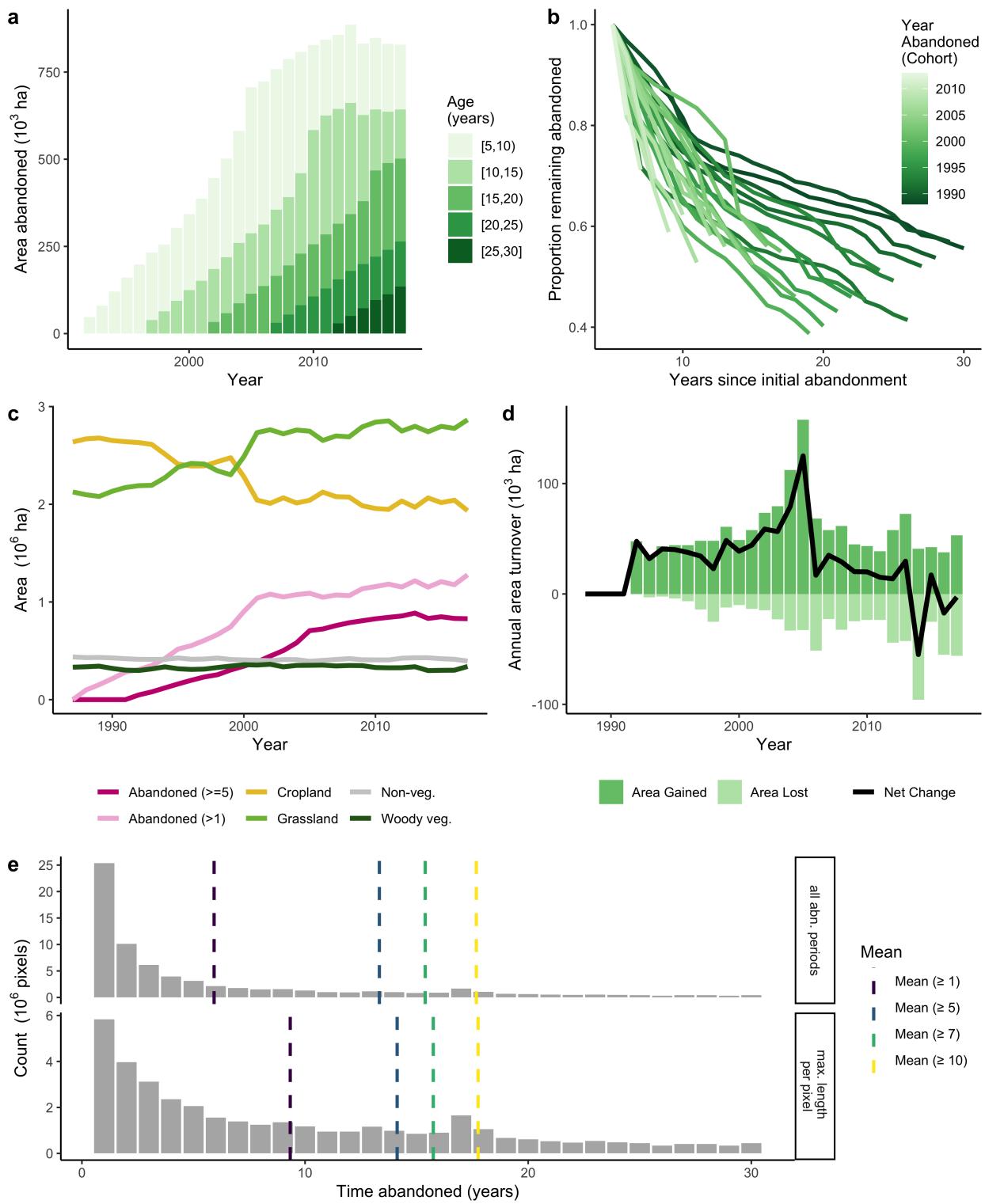


Figure S36: Abandonment patterns for Volgograd, Russia, following Figure S27.

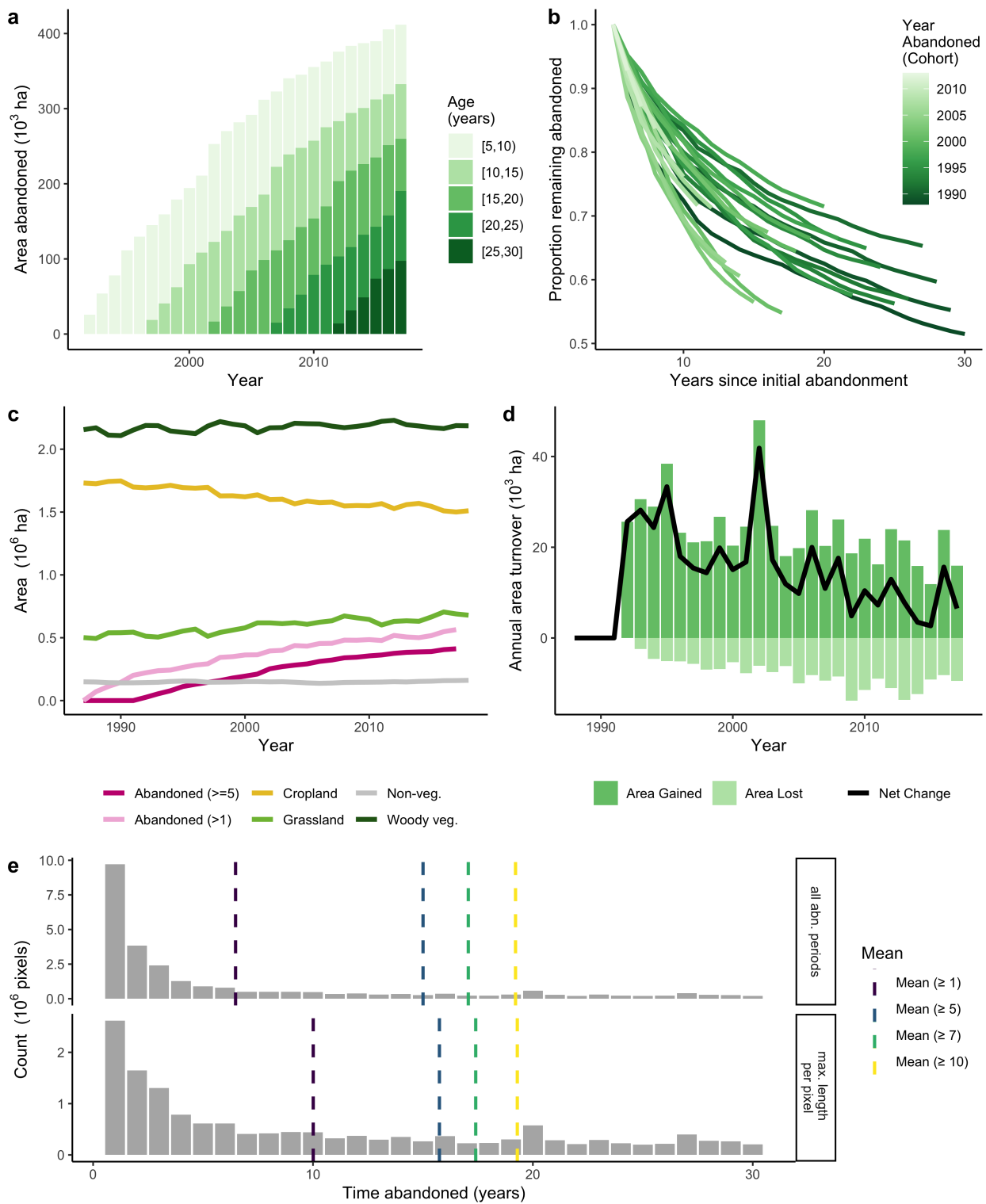


Figure S37: Abandonment patterns for Wisconsin, USA, following Figure S27.